1.

Past and Possible Future Earthquakes of Significance to the San Diego Region

John G. Anderson, M.ERRI, Thomas K. Rockwell, and Duncan Carr Agnew

The potential for earthquakes that may significantly affect the San Diego, California, region is examined from the viewpoint of geology, seismic history, and strong ground motion. We have compiled the best available data on slip rates and recurrence times for all major faults in southern California and northern Baja California, identified possible fault segments that might rupture in single earthquakes and obtained repeat times for these events which are consistent with (or at least not contradicted by) trenching studies. The most important faults for San Diego's seismic hazard are the Rose Canyon fault, the Elsinore fault, and faults immediately offshore (Coronado Banks, San Diego trough). There have not been any major earthquakes on any of these nearby faults in historical time, but the geological evidence is clear that such events will eventually occur.

San Diego is located on the western flank of the Peninsular Range batholith, and there is weak evidence that attenuation in this batholith might be lower than average for California. We combine the geological data with an attenuation model to obtain an estimate for the occurrence rate of various levels of peak ground acceleration in downtown San Diego from events with moment magnitude greater than about 6. We find that peak accelerations of 10% g to 20% g are expected about once every 100 years. There are considerable uncertainties in this estimate, but nevertheless, strong ground shaking from a magnitude 6.0 or greater earthquake near the populated area would not be a scientific surprise.

---

[1]Seismological Laboratory, Mackay School of Mines, University of Nevada - Reno, Reno, Nevada 89557 (JGA)

[2] Institute of Geophysics and Planetary Physics, Scripps Institute of Oceanography, University of California, San Diego, La Jolla, CA 92093. (DCA, formerly JGA)

[3] Department of Geology, San Diego State University, 5402 College Avenue, San Diego, CA 92115. (TR)

INTRODUCTION

The city of San Diego, California, is the seventh largest in the United States, with a population of 1,013,000 at the start of 1987; San Diego County (which includes the metropolitan region), had a population of 2,166,000 and was growing at 2.6% per year (4500 new residents per month). The adjacent city of Tijuana, Mexico had a population somewhere between 800,000 and 1,000,000, and a growth rate of about 5.6% per year (Herzog, 1986). Thus over 3,000,000 people are exposed to the earthquake hazard in the overall metropolitan area - which also has a major U.S. Navy base, and important aerospace, high-technology, and tourist industries.

To date, fortunately, the San Diego - Tijuana metropolitan region has been spared a major local earthquake, though it is often rattled by more distant events. This good luck cannot be expected to last forever, since at least one active fault (the Rose Canyon) bisects San Diego (Figure 1); while this and other nearby faults have not caused large earthquakes in historical time (post-1770), eventually one of them will. In addition, more distant faults (such as the San Andreas) might generate earthquakes strong enough to produce significant damage in the area.

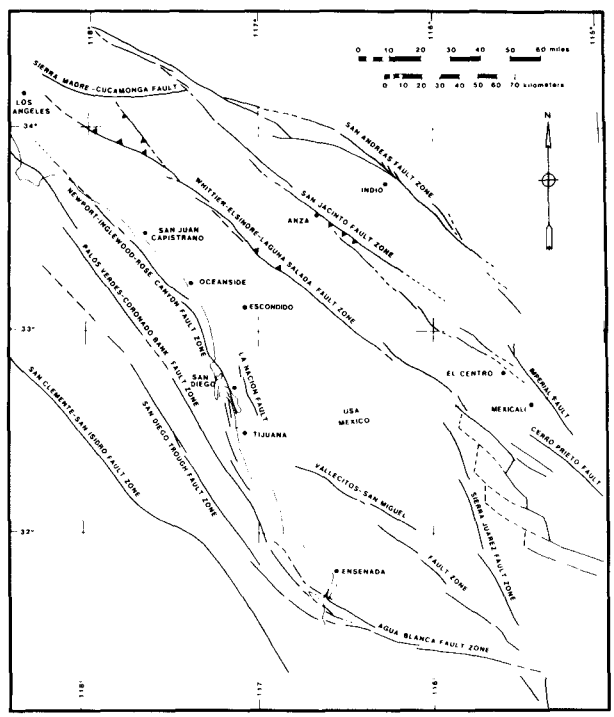

Figure 1 - Major faults in the San Diego region.

This paper summarizes the major faults that might affect the San Diego region, tabulates significant historical earthquakes, and uses geological information to identify potential fault ruptures that might cause significant earthquakes in the future. In addition, it examines the strong ground motion records from the San Diego region and identifies regional concerns with the estimation of ground motions from future events.

GEOLOGICAL CONSIDERATIONS

To discuss the seismicity, we use geological information to assess the average late Quaternary slip rate and characteristic size of earthquakes on active faults near San Diego (Figure 1). From east to west these faults are the San Andreas fault, the Imperial and Cerro Prieto faults of Imperial Valley, the San Jacinto fault system, the Whittier - Elsinore - Laguna Salada fault system, the Vallecitos - San Miguel fault zone, the Newport-Inglewood - Rose Canyon fault zone, the Agua Blanca and Palos Verdes - Coronado Bank fault zone, the San Diego Trough fault zone and the San Clemente - San Isidro fault zone. Most of the above have a dominantly dextral sense of slip, and all comprise portions of dextral fault zones. The principal exception is the Laguna Salada fault, which has about twice as much vertical as horizontal slip.

These long fault zones are unlikely to rupture in a single earthquake; along all of them are places where the mapped surface faults step to the left or right, bend, change their sense of slip (e.g., by adding normal or reverse motion), or cannot be mapped continuously. The segmentation hypothesis (Schwartz & Coppersmith, 1984, 1986) holds that these places are surface expressions of deep-seated obstacles to rupture. We have used these features to identify possible segments in each zone; we consider these segments to be most likely to rupture in single earthquakes. The segments, and the bases of their identification, are listed in Table 1 and identified on Figure 2. Segment boundaries were chosen as major steps (>3 km) and bends in the fault, or at the end points of historical ruptures. In many historical earthquakes, however, multiple segments have ruptured in one earthquake; we account for this possibility later in the paper on a fault by fault basis.

Table 1

Rational for fault segment boundaries on the more active faults in Southern California and northern Baja California.*

Fault Segment	Rational
San Andreas	
1. Indio	Southern end defined by step-over to Brawley seismic zone, Northern end approximated at San Gorgonio bend
2. Palmdale	Southern end defined by San Gorgonio bend Northern end defined by Big Bend near Fort Tejon (Sieh, 1984). Probable rupture of 8 Dec. 1812 earthquake (Jacoby et al, 1986)

3. 1857	Multiple segments. Historical 1857 rupture. (eg. Sieh, 1978b)
Cerro Prieto Fault	
4. 1934	Multiple segments. Historical 1934 rupture (e.g. Anderson & Bodin, 1987).
Imperial Fault	
5. 1940	Multiple segments. Historical 1940 rupture (e.g. Anderson & Bodin, 1987).
San Jacinto Fault	
6. Superstition Hills/Mountain	Entire mapped surface trace of fault. Really two faults, subparallel, same length, treated as one here for simplicity.
7. 1968	Extent of rupture in 1968 Borrego Mountain earthquake (Clark, 1972).
8. Coyote Mtn.	Mapped surface extent of fault bounding southwest side of Coyote Mtn.
9. 1954	Extent of seismic rupture, 1954 earthquake (Sanders, 1986)
10. Clark Valley	Southern extent: 1954 earthquake (Sanders, 1986) Northern extent: 1937 earthquake (Sanders, 1986)
11. Anza	Southern extent: 1937 earthquake (Sanders, 1986) Northern extent: 1899 earthquake (Sanders, 1986)
12. 1899	Approximate extent of seismic rupture, 1899 earthquake (Sanders, 1986).
13. 1918	Approximate extent of known seismic rupture, 1918 earthquake (Sanders, 1986).
14. 1923	Approximate extent of seismic rupture, 1923 earthquake (Sanders, 1986).
Elsinore- Laguna Salada	
15. Sierra Mayor	Several sub-parallel segments bounded by right steps (Mueller & Rockwell, 1984)
16 Chupamiertos	Southern extent: Sierra Mayor segments Northern extent: Canyon Rojo/Laguna Salada fault (Mueller & Rockwell, 1984) The instrumental epicenter for the Dec. 30, 1934 Earthquake (M6.5) is near this fault segment (Leeds, 1979).
17. Laguna Salada	Extent of surface rupture, 1892 earthquake (Mueller & Rockwell, 1984)
18. Coyote Mountain	Southern extent: Yuha basin where surface trace loses expression. Northern extent: Tierra Blanca mountains where fault makes a left step.
19. Julian	Southern extent: Tierra Blanca mountains where fault makes a left step. Northern extent: Agua Tibia-Palomar Mountain where fault makes a left bend and becomes a thrust fault.
20. Temecula	Southern extent: Agua Tibia- Palomar Mountain Northern extent: Lake Elsinore where fault makes a major right step.
21. Glen Ivy	Southern extent: Lake Elsinore Northern extent: Temescal Valley where fault makes a major right bend (Millman and Rockwell, 1986). Probable source segment of May 15, 1910 earthquake (Rockwell et al, 1986).
22. Whittier-Chino	Southern extent: Temescal Valley bend Northern extent: Transverse ranges.
San Miguel - Vallecitos Fault Zone Trend	
23. Southern	Multiple breaks for the 1954-56 earthquake swarm (Shor & Roberts, 1958)
24. Central	Southern extent: major right step to the 1954/56 earthquakes Northern extent: major right step to northern segment.

25 Northern	Southern extent: major right step to the central segment. Northern extent: End of mapped surface trace of fault.
Rose Canyon - Newport Inglewood Fault Zone	
26. Descanso	Southern extent: Juncture with Coronado Bank - Agua Blanca fault near Punta Descanso Northern extent: Major right step in San Diego Bay
27. Mission Bay	Southern extent: major right stĕp at San Diego Bay Northern extent: left bend at Mount Soledad
28. La Nacion	Extent of mapped fault
29. Del Mar	Southern extent: left bend at Mount Soledad Northern extent: structural complexities/step near Oceanside.
30. Camp Pendleton	Southern extent: structural complexities near Oceanside. Northern extent: approximate southern extent of 1933 earthquake aftershock zone.
31. 1933	Extent of seismic rupture in March 10, 1933 earthquake.
Agua Blanca- Coronado Bank fault zone	
32. Valle Trinidad	Eastern extent: Juncture with San Pedro Martir fault zone. Western extent: major right step in Valle Agua Blanca. (Rockwell et al 1987).
33. Santo Tomas	Eastern extent: Valle Agua Blanca. Western extent: major right step/bend in Valle Santo Tomas. (Rockwell et al 1987).
34. Punta Banda Ridge	Eastern extent: Valle Santo Tomas Western extent: right step at Estero (Rockwell et al., 1987)
35. Offshore	Multiple potentially long segments. Offshore structures are poorly defined (Legg, 1985).
San Diego Trough Fault Zone	
36. Offshore	Multiple potentially long segments. Offshore structures are poorly defined (Legg, 1985).
San Clemente - San Isidro fault zone	
37. Offshore	Multiple potentially long segments. Offshore structures are poorly defined, however a large left bend suggests potentially large earthqakes (Legg, 1985).
Sierra Madre- Cucamonga & related central Transverse Ranges faults	
38.	Multiple segments. Feb 9, 1971 San Fernando earthquake is probably characteristic.

* Potential references for each fault are numerous, so we have listed only a few.

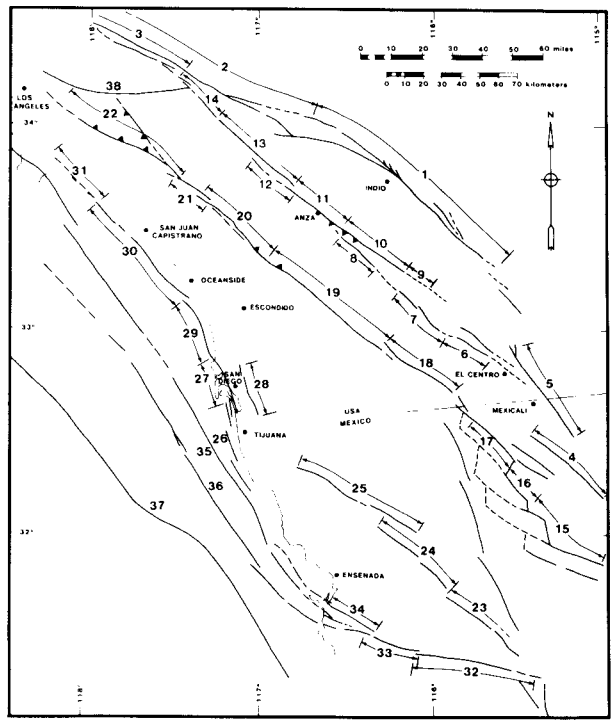

Figure 2 - Segmentation of major faults. Segment boundaries are major disruptions in the continuity of the faults, and thus represent likely end points for rupture during major earthquakes.

To estimate earthquake occurrence rates from geological data we need to know both the extent of rupture (to estimate the possible earthquake magnitude) and the slip rate and extent to which this slip is relieved by aseismic creep (to estimate recurrence rates). In the remainder of this section we summarize some of the geological evidence for rates of Holocene activity, and the basis for slip rate and earthquake recurrence rate estimates for each fault. Wesnousky (1986) has also recently compiled a table of slip rates on faults in California; our results are generally consistent, with differences attributable to differing judgement or new data. Within uncertainties our slip model is consistent with plate tectonic constraints (DeMets et al., 1987). Our results are summarized in Table 4.

San Andreas Fault

The San Andreas is one of the best studied faults in California. The slip rate on this fault is about 35 mm/yr in the Carrizo Plain (Sieh and Jahns, 1984), but appears to decrease to about 25 mm/yr at Cajon Creek (Weldon and Sieh, 1985). Near Indio, in the Coachella Valley, Sieh (1986) has determined a rate of about 30 mm/yr based on offset late Holocene lacustrine beach deposits.

Studies of the prehistoric earthquake history of this fault led Sieh (1978a, 1984) to conclude that the section of the fault at Pallet Creek (near Palmdale) had large earthquakes, on the average, about every 145 years. This section of the fault last broke in 1857 with the great Fort Tejon earthquake (M 8.25), which produced 9 m of lateral slip in the Carrizo Plain (Sieh, 1978b). Given the 35 mm/yr slip rate in the Carrizo Plain, an event of this size would be expected every 300 years. The 145-year recurrence interval at Pallet Creek may reflect rupture overlap between the segment that broke in 1857 and the Mojave segment, which apparently broke in 1812 (Jacoby et al., 1987) (Figure 1). This is reasonable since in the 1857 earthquake the fault slip near Palmdale was considerably lower than in the Carrizo Plain (Sieh, 1978b).

The southern San Andreas has a high probability for a major earthquake in the near future, based on statistical analyses of the fault's paleoseismic record (Sykes and Nishenko, 1984; Wesnousky, 1986). Weldon and Sieh (1985) estimated a recurrence time of about 250 years for large earthquakes along the San Andreas fault at Cajon Pass, with the last earthquake possibly being in the early 18th century (250 years ago). This last earthquake, however, was probably the 1812 earthquake that Jacoby et al. (1987) delineated at Wrightwood, just to the northwest along the fault. The last earthquake at Sieh's Indio site occurred about 300 years ago during the last high-stand of ancient Lake Cahuilla (Sieh, 1986) suggesting that only a relatively short portion (±100 km) of the San Andreas ruptured in 1812 (Segment 2? on Fig 2). Potentially, then, the next southern San Andreas earthquake may rupture only the Indio segment (Segment 1). Alternatively, since there has been 130 to 175 years for strain to accumulate along segment 2, a large earthquake could possibly break from the Salton Trough through the section that broke in 1812. The in-between section of the fault near San Gorgonio Pass, however, is structurally complex and it is not clear whether there is surface rupture associated with large earthquakes there.

San Jacinto Fault

The paleoseismic history and slip rate of the San Jacinto fault are not as well determined as that of the San Andreas fault, though many studies are in progress that will clearly indicate its potential and probable future activity. Sharp (1981) determined a minimum mid-Quaternary to present slip rate of 8-12 mm/yr for the central part of the fault near Anza (segment 11). A decrease in rate along the San Andreas fault south of the junction between it and the San Jacinto fault may

simply reflect a transfer of slip to the San Jacinto. Sharp (1981) suggested that trenching studies along the Coyote Creek fault (segment 7) in the Imperial Valley imply a lower slip rate from mid-Holocene to the present. However, recent studies of folded mid-Quaternary lacustrine and fluvial deposits in the San Felipe Hills (segment 9 and to the southeast) demonstrate Quaternary slip along the buried projection of the Clark fault (Feragan, 1986; Wells, 1987), thereby negating Sharp's evidence for variable rates of slip.

Studies of offset late Quaternary alluvial fans and terrace deposits near Anza indicate a minimum of 8-10 mm/yr since the early Holocene and 12-14 mm/yr since the late Pleistocene (Rockwell et al., 1986; Rockwell et al, 1988, submitted for publication). This section of the fault (Segment 11) has been called the Anza Seismic Gap by Sanders and Kanamori (1984) because of its lack of known historical earthquakes (since 1890) and its low level of microearthquake activity.

Elsinore Fault

The Elsinore fault zone is one of the longest in southern California, stretching over 260 km from the Los Angeles Basin southeasterly across the International Border into Mexico as the Laguna Salada fault (Lamar and Rockwell, 1986). Recent studies along the fault suggest a slip rate of 5-6 mm/yr between Corona and Lake Elsinore (Millman and Rockwell, 1986), 5±2 mm/yr at Agua Tibia Mountain (Vaughan, 1987; Vaughan and Rockwell, 1986), and a minimum of 4.5 ±1 mm/yr in the Coyote Mountains near the International Border (Pinault and Rockwell, 1984).

Trenching studies at Glen Ivy Marsh in Temescal Valley (segment 21), located in the same area as the Millman and Rockwell study, indicate a recurrence interval for ground-breaking earthquakes of about 200 years (Rockwell et al., 1986). The most recent earthquake to rupture the surface at Glen Ivy was the May 1910 Temescal Valley earthquake (Toppozada and Parke, 1982), with magnitude near 6. This earthquake apparently displaced a cement flume by about 35 cm laterally (Brake and Rockwell, 1987; Brake, 1987). A study of displacement during a circa 1300 A.D. earthquake indicates at least 50 cm of slip from it (Brake and Rockwell, 1987). This 15-20 km section of the Elsinore fault thus appears to be characterized by moderate earthquakes in the M=6 to M=6.5 range.

In the Coyote Mountains (segment 18), Rockwell and Pinault (1986) studied progressively older displaced late Holocene channel bars, channel walls, channels, and other geomorphic features, and suggested displacements of 80 to 185 cm per event, corresponding to about M 6.5 to M 7 size events. Pinault and Rockwell (1984) suggested a recurrence interval of about 350 years for these events, with the last event being prehistoric.

The Laguna Salada fault (segment 17) has also suffered repeated Holocene surface rupture with oblique-slip events measuring up to 5 m each (Mueller and Rockwell, 1984; Mueller, 1984). The last earthquake

along this section of the fault produced up to 5 m of vertical slip, with probably less than half of that amount horizontally (Mueller, 1984). The rupture cuts completely unweathered and unconsolidated alluvium, and free faces still punctuate much of its length. A large earthquake struck southern California and northern Baja California on February 24, 1892, producing intensity VII damage in San Diego (Toppozada et al., 1981; Strand, 1980). Strand places this earthquake on the Laguna Salada fault whereas Toppozada et.al. place it to the west where there is no known late Quaternary faulting. Part of the placement problem rides on the lesser damage at Yuma than at San Diego, possibly explained by attenuation across the thick fill of the Salton Basin. The data for a very recent and probably historical earthquake along the Laguna Salada fault led Mueller and Rockwell (1984) to agree with Strand's interpretation. Another earthquake, the 1934 M 6.5 event, may account for part of the displacement but this earthquake was instrumentally estimated to have been farther to the south, possibly along the Chupamiertos segment of the fault zone (segment 16).

Based on a comparison between the Elsinore and San Jacinto faults on four different criteria, we conclude that the geological slip rate of about 5 mm/yr on the Elsinore fault is reasonable. The geological slip rate is about 2 to 3 times greater on the San Jacinto fault. The occurrence rate of small earthquakes (M 3.0 to 3.9) from 1934 to 1980 was also about 2.5 times greater on the San Jacinto fault (Anderson, 1983,1984), consistent with the geological estimates. Figure 4 shows that since 1932, the San Jacinto fault has had at least five times as many $M > 5$ earthquakes. The lower rate of the largest earthquakes can be understood if, as we suggest in Figure 2 and Table 1, the Elsinore zone has larger segments which produce larger, and thus less frequent, earthquakes than the San Jacinto zone. On the other hand, the geodetic strain rate is five times greater on the San Jacinto fault than the northern Elsinore fault, and shows a regional peak over the San Jacinto fault but not the northern Elsinore fault (segments 21 and 22 of Figure 2), King & Savage (1983). This low geodetic strain rate contradicts the geological slip rate estimate; a possible explanation is the nonlinearity in the cycle of seismic strain accumulation and release (Thatcher, 1983), with this section of the Elsinore fault being late in the cycle.

The Sierra Juarez fault zone is the main fault bounding the west side of the Salton Trough south of the international border. However, based on its relatively high sinuosity and lack of expression of recent faulting, it does not appear to have been active in the late Quaternary. Therefore this fault zone is not considered further.

Inner Borderland Faults

In the offshore region (the inner part of the Southern California Borderland) we know much about the locations of faults (from seismic reflection profiling) but very little about their activity. This region is characterized by a complex system of anastomosing faults that include the San Clemente-San Isidro, San Diego Trough, Coronado Bank-Palos Verdes, and Rose Canyon/ Newport-Inglewood trends (Legg, 1985; Legg and Kennedy, 1979; Kennedy and Welday, 1980: Greene and others, 1979). The San Diego Trough and Coronado Bank fault zones trend onshore as the Agua Blanca fault (Legg, 1985), although slip from the Agua Blanca zone may also feed the Rose Canyon fault via unnamed faults identified as segment 26 in Fig 2 (Rockwell et al., 1987). Onshore study of the Agua Blanca fault indicates that about 6 mm/yr of dextral slip is distributed among three faults that trend offshore to connect with the inner borderland faults (Rockwell et al., 1987; Schug, 1987; Hatch, 1987). The main Agua Blanca fault (segment 34) accounts for most of this, with at least 4 mm/yr of late Quaternary slip; the secondary fault shown south of segment 34 takes up about 1±0.6 mm/yr. These faults collectively comprise the Coronado Bank fault zone to the northwest.

The San Diego Trough fault appears to receive slip from only a minor southern strand of the Agua Blanca fault onshore in Baja California (Legg, 1985), which has a very poor geomorphic expression onshore as an active fault and probably has no more than 1 mm/yr of slip associated with it (Rockwell et al., 1987). The San Clemente fault appears to connect with the San Isidro fault to the southeast and does not come onshore in Baja California (Legg, 1985). Based on offset submarine strata and geomorphic features such as canyons and fans, Legg (1985) attributes at least 4 mm/yr of slip to this fault zone.

Another important feature is the San Miguel fault zone, which historically has been the most active fault in northern peninsular Baja California. Six M 6-6.8 earthquakes occurred as a swarm in 1954 and 1956 along its southern length. The total offset of Cretaceous and Miocene rocks on this fault zone is estimated to only be about 500 m (Harvey, 1986), suggesting either a very low slip rate or recent inception of faulting. With present data either is plausible, so the slip rate estimated for the inner borderland faults from the Agua Blanca fault must be considered a minimum, since slip from the San Miguel trend must also feed into the coastal faults (even though a recognized surface link is lacking).

These data indicate that a minimum of 5 mm/yr is distributed between the Coronado Bank and Rose Canyon faults in the vicinity of San Diego, with as much as 10 mm/yr when the San Clemente fault zone is added. Although data are not presently available as to how the Agua Blanca slip is partitioned, it is clear that the Coronado Bank and Rose Canyon faults together comprise the greatest seismic hazard to the San Diego - Tijuana region because they are so nearby. These two faults are active at the microearthquake level. Simons (1977) relocated earthquakes in a limited area centered on San Diego for the years 1934 to 1974. He found at least 10 earthquakes, out of 37 with magnitudes between 2.3 and 3.7,

that could be considered, within location accuracy, to have occurred on the main trace of the Rose Canyon fault. He also found six events which could plausibly be located on the La Nacion fault. The remaining events were mostly in the immediate offshore no farther than the Coronado Banks fault. In the summers of 1985 and 1986, microearthquake swarms were located below San Diego Bay (Reichle et al., 1985). The largest event in this series was the October 29, 1986 earthquake (M_L=4.7), located near the south end of San Diego Bay. These events confirm that the Rose Canyon fault is active.

The geomorphic evidence for recent activity on the Rose Canyon fault includes the persistence of San Diego Bay, which is a depression caused by sagging between the Rose Canyon and La Nacion faults, and Mt. Soledad, a local topographic high apparently caused by the left bend in the fault. The on-land portion of the fault is completely urbanized, so that Holocene geomorphic evidence of activity is obscured. The slip rate on the Rose Canyon fault is not well determined. A slip rate of 1-4 mm/yr can be derived from the data in Kennedy (1975). Based on interpretation of 1929 aerial photographs of the Rose Canyon fault zone near Mount Soledad, West (1987) suggested a late Quaternary rate of about 1.2 mm/yr. We believe that this rate is reasonable based on the convincing evidence that close to 5 mm/yr is distributed between the Coronado Banks and Rose Canyon fault zones. The seismic evidence for similar activity rates on these two faults at the microearthquake level also supports this rate.

HISTORICAL SEISMICITY

The historical record of earthquakes is as good for San Diego as for any other part of California. For intensity high enough to cause serious damage (VII or above) the record is probably complete from 1770, when the mission and presidio were established. As is generally true for the Hispanic period of California, reporting of milder shaking was unusual. The quality of reporting became much better in 1850 when an Army post was established; weather records from this (and later from the Weather Bureau) give a fairly complete listing of felt earthquakes. Additional descriptive material can be found in newspaper reports, which are also fairly complete: the San Diego **Herald** ran from 1851 through 1859, and the **Union** from 1869 through the present. For the 1860's another important source is the manuscript notes of Benjamin Hayes, now in the Bancroft Library (Agnew et al., 1979).

It is important to realize that this completeness of coverage in the San Diego area does not imply an ability to locate the earthquakes reported. This can be done only from a wide distribution of felt reports; for San Diego these are never available from the west, and only occasionally from the south. For many important historical earthquakes, the location and magnitude cannot be determined.

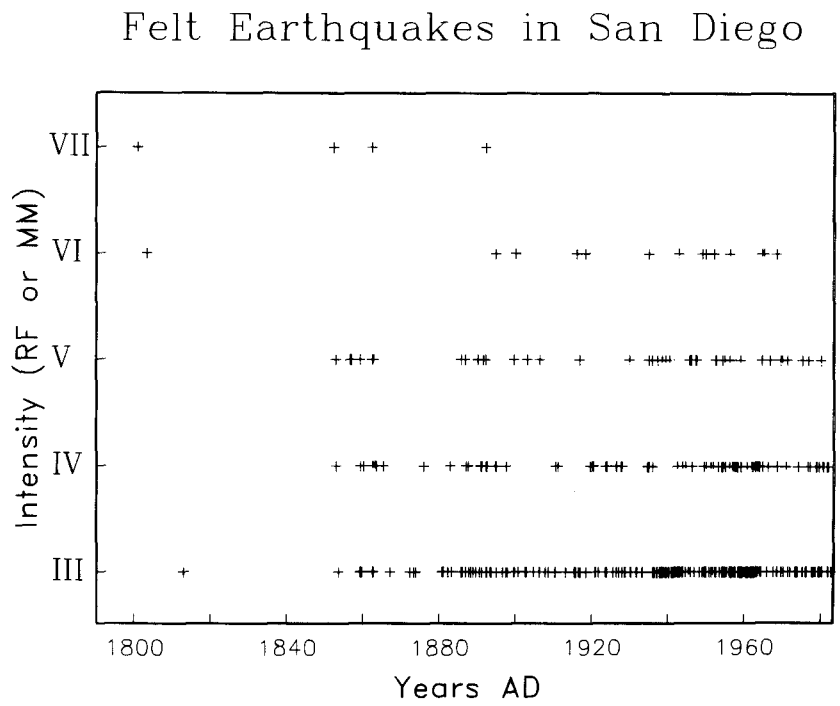

Figure 3 - Intensities of felt earthquakes in San Diego.

Figure 3 shows all intensities reported for San Diego through the end of 1982. (Intensity III was used for cases where an earthquake was simply reported as "felt".) This shows the increasing completeness of coverage with time, and also that the strongest shaking experienced in San Diego occurred in the 19th century - one reason why the earthquake hazard there is currently regarded as low. Table 2 lists the more important (intensity V or above) earthquakes before 1934. Later ones are listed in Table 3. Table 2 has been drawn from the more complete list in Agnew et al. (1979), which should be consulted for sources. Some of the intensities have been changed to the values determined by Toppozada et al. (1981). The more notable of the earthquakes in this table are:

1800 November 22.

Adobe walls at the Presidio of San Diego were damaged, and the walls of the new church at San Juan Capistrano (then under construction) were cracked.

1803 May 25.

The mission church at San Diego was damaged slightly.

1852 April 12.

The local newspaper report said that an "adobe house, with a tiled roof, situated near the Plaza at Old Town, was destroyed by" a "very severe shock" that "continued some thirty seconds". This earthquake is not mentioned in any other source, nor is any other damage described. It is therefore hard to know if this report actually reflects an earthquake; if it does, the damage must reflect especially poor construction.

1862 May 27.

This earthquake (Legg and Agnew, 1979) appears to have been closer to San Diego than any other damaging event, and also to have caused the strongest shaking (with the possible exception of the 1800 earthquake). It had a long aftershock sequence, felt more completely at San Diego than in Los Angeles; this, in addition to the fact that the mainshock was not felt at Yuma, suggests a location to the south or west. Cracking was reported in the adobe houses in Old Town and the brick lighthouse on Point Loma (though no glass was broken). Earthfalls from bluffs on Point Loma may have caused a small wave in San Diego Bay.

1892 February 23.

This earthquake caused widespread minor damage (including cracked plaster) in San Diego. As noted above, its location is uncertain, largely because of the paucity of reports from Baja California and the Colorado Desert. Toppozada et al. (1981) located the epicenter in the southeast corner of San Diego County; Strand (1980) places it farther to the east, and somewhat south (possibly, as described above, on the Laguna Salada fault) which also makes it larger (magnitude 7½).

1894 October 23.

Though this earthquake also caused some damage in the San Diego area, it was less strong than the 1892 event. It seems to have been definitely located in the mountains east of San Diego, but again the lack of intensity data from Mexico makes the north-south position unclear.

Two earthquakes are notable for the lack of significant damage in San Diego:

1812 December 8.

This earthquake (possibly on the San Andreas fault (Jacoby et al., 1987)), was felt in San Diego but caused no damage there, though it was damaging in San Gabriel and caused the collapse of the church at San Juan Capistrano (Toppozada et al, 1981).

1857 January 9.

This was a magnitude 7.9 earthquake on the San Andreas fault, rupturing from near Cajon Pass to Parkfield (Figure 2). The intensity in San Diego was V with "considerable alarm" and many people fleeing from buildings; the only damage was that "several articles of merchandise were thrown from the shelving" and some plaster was cracked (Agnew and Sieh, 1978).

Table 2

Preinstrumental Earthquakes Causing Intensity V+ Shaking in San Diego

Local Date	Intensity	Location	Magnitude
1800 November 22	VII?	?	
1803 May 25	VI?	?	
1852 April 12	VII?	? [*Fabulous*?]	
1852 November 29	V	Mexicali Valley	
1856 September 20	V	Santa Ysabel?	
1857 January 9	V	Fort Tejon	7.9
1859 March 25	V?	Nearby?	
1862 May 27	VII	Nearby?	
1862 May 29	V?	Nearby?	
1862 June 13	V?	Nearby?	
1862 October 21	V?	?	
1885 September 13	V	?	
1886 October 8	V	?	
1890 February 5	V	?	
1890 February 9	V	San Jacinto?	6?
1891 July 30	V	Colorado Delta	7??
1892 February 23	VII	Northern Baja?	6¾
1892 February 24	V	Northern Baja?	
1894 October 23	VI	East county?	5½
1899 July 22	V	Cajon Pass	6½
1899 December 25	VI	San Jacinto	6½
1903 January 23	V	Colorado Delta	7
1906 April 18	V	Imperial Valley	6
1915 November 20	VI	Mexicali Valley	7.1
1916 September 29	V	East county?	
1918 April 21	VI	San Jacinto	6.8
1929 December 2	V	Northern Baja	

Table 3

Listing of earthquakes with strong motion records from within San Diego, Jan. 1, 1932–Sept. 24, 1986

Caltech Catalog: basis of determining locations, times, magnitudes

year mo-d	hrmn	lat.	long.	M_L	dist.[1]	a_{max}[2]	MMI	a_{max} obs.[3] z	e	n	completeness[4]
1934 12-30	13:52	32.280	-115.460[6]	6.5	165.7	8.9	?	-4-	-4-	-4-	vl
1934 12-31	18:45	32.140	-114.950[6]	7.1	216.1	7.1	?	-8-	-8-	-8-	l-vl
1937 03-25	16:49	33.465	-116.415[5]	6.0	107.4	14.4	IV-V	3.7	9.0	10.4	l
1939 05-01	23:53	32.000	-117.500	5.0	86.4	11.4	V	2.	2.	3.	vl
1939 06-24	16:27	32.000	-117.500	5.0	86.4	11.4	III	2.	4.	5.	l-vl
1940 05-19	04:36	32.733	-115.500	6.7	154.7	11.3	IV-V	2.	5.	4.	vl?
1942 10-21	16:22	33.049	-116.088[5]	6.5	105.6	19.7	VI	9.	14.	18.	c
1943 08-29	03:45	34.267	-116.967	5.5	172.4	4.6	IV	2.	3.	2.	vl
1945 08-15	17:56	33.217	-116.133	5.7	109.6	11.7	V	1.	5.	3.	l
1947 04-10	15:58	34.983	-116.550	6.2	257.0	2.8	V	1.	2.	2.	
1948 12-04	23:43	33.933	-116.383	6.5	152.1	10.4	VI	-	9.	10.	l
1949 11-04	20:42	32.180	-116.520[6]	5.7	84.2	17.7	VI	12.	13.	17.	l
1951 12-26	00:46	32.817	-118.350	5.9	112.9	12.5	VI	3.	11.	14.	c
1952 07-21	11:52	35.000	-119.017	7.7	305.0	4.2	V	1.	5.	4.	vl?
1954 03-19	09:54	33.296	-116.176[5]	6.2	111.0	15.3	V	3.	16.	13.	c
1954 10-24	09:44	31.730	-115.920[6]	6.0	159.6	7.2	V	2.	3.	3.	vl?
1954 11-12	12:26	31.770	-115.970[6]	6.3	153.1	9.2	V	3.	7.	4.	l
1956 02-09	14:32	31.750	-115.917	6.8	158.8	11.4	VI	7.	12.	14.	c
1956 02-14	18:33	31.500	-115.500	6.3	207.1	5.0	V	3.	5.	5.	vl
1956 02-15	01:20	31.500	-115.500	6.4	207.1	5.2	V	5.	6.	7.	vl
1964 12-22	20:54	31.811	-117.131	5.6	100.8	12.7	VI	11.	24.	32.	l
1968 04-09	02:28	33.190	-116.129	6.4	108.6	17.8	VI	12.7	28.9	29.5	c
1971 02-09	14:00	34.411	-118.401	6.4	220.0	4.6	VI	3.	6.	6.	l
1979 10-15	23:16	32.614	-115.318	6.6	172.3	8.7					
Coronado 1770 Ava. del Mundo								*	*	*	?
Coronado 1780 Ava. del Mundo								*	*	*	?
El Capitan Dam left abutment								*	*	*	?
San Diego SDGE Office Bldg.								*	*	*	?
1980 02-25	10:47:38.5	33.501	-116.513	5.5	104.9	11.2					
El Capitan Dam left abutment								-80-	-80-	-80-	
Poway								*	*	*	
San Diego SDGE Office Bldg.								*	*	*	
1985 05-08	23:40	31.890	-115.821	5.0	155.8	4.2					
? are there any?											
1986 07-08	09:20	33.998	-116.606	5.6	150.4	6.4					
Palomar Mountain 330					75.5	19.6		30.	30.	30.	vl
Puerta La Cruz 168					75.5	19.6		60.	60.	60.	c
Poway City Hall 499					122.8	9.2		20.	40.	60.	l-vl
San Diego Murray Dam 470					141.2	7.2		10.	20.	30.	l
Oceanside 333					111.1	10.8		not triggered			
Alpine 467					129.3	8.4		not triggered			
San Diego Murray Hill 027					140.5	7.2		not triggered			
Ocean Beach 121					150.7	6.3		not triggered			
San Diego SDGE Bldg. 300					151.2	6.3		not triggered			
1986 07-13	13:47	32.971	-117.870	5.3	72.8	17.4					
note: reduced with nominal 18.3 mm/g, all ±5 gal or more											
Ocean Beach 121					63.7	20.9		48.	94.	75.	c
San Diego SDGE Bldg. 300					71.7	17.8		25.	30.	48.	l
San Diego Murray Dam 470					79.9	15.2		20.	25.	20.	vl
Oceanside 333					56.3	24.7		10.	19.	27.	vl
Poway City Hall 499					77.4	15.9		48.	70.	100.	c
Palomar Mountain 330					102.9	10.3		13.	15.	12.	vl
Puerta La Cruz 168					117.2	8.4		16.	25.	20.	vl
Alpine 467					107.9	9.6		not triggered			
San Diego Murray Hill 027					78.3	15.7		not triggered			
1986 10-29	02:38	32.616	-117.134	4.7	11.6	93.3					
San Diego SDGE Bldg. 300					11.6	93.3		80.	50.	60.	pc
San Diego Murray Dam 470					20.1	57.1		20.	10.	10.	vl
Poway City Hall 499					38.6	28.0		10.	10.	xx.	vl

[1] Distance from 32.72°N, -117.15°W

[2] Predicted by Joyner & Boore (1981)

[3] An asterisk (*) indicates that the instrument triggered but ground motions are too small to be reliably measured. A dash on either side of the number indicates a single peak was given in the source for all 3 components, and that a copy of the original was not inspected.

[4] c = complete S wave; l = late trigger; vl = very late trigger; p = significant part of P-wave on record

[5] Relocation by Sanders et al. (1986).

[6] Relocation by Leeds (1979).

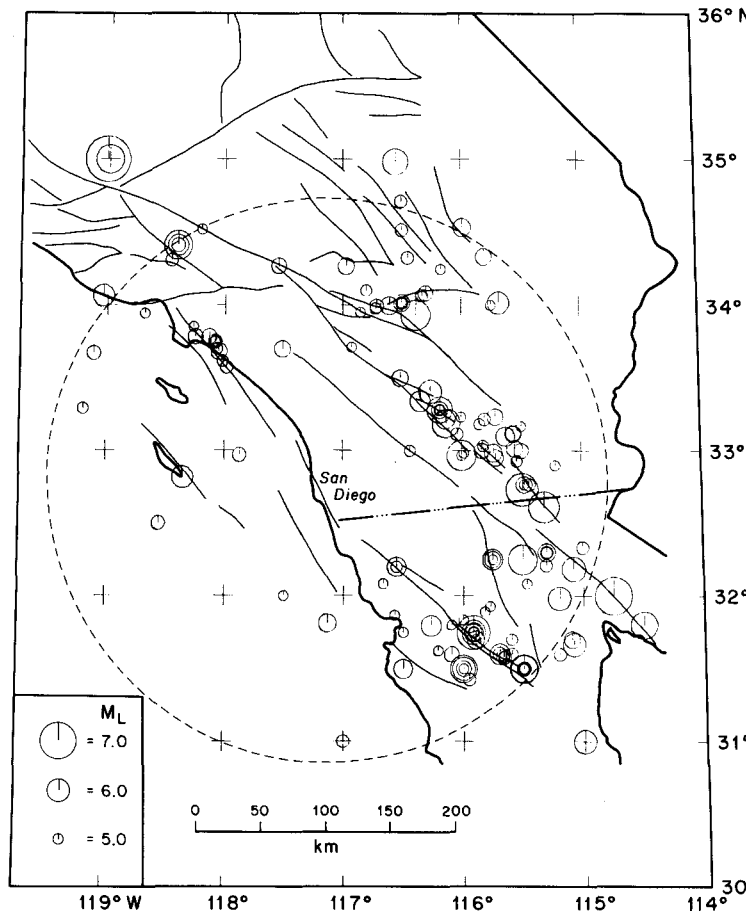

Figure 4 - Major faults and epicenters of all earthquakes listed in Appendix I. Inside the circle, all earthquakes with M_L>5.0 from the Caltech catalog, Jan. 1, 1932 to Sept. 24, 1986 are shown. Outside the circle, only earthquakes that cause peak acceleration of greater than 2 cm/sec^2 (according to Joyner and Boore's 1981 regression) have been included.

Since the beginning of earthquake records, San Diego has been surrounded by large earthquakes, but none have been nearby. For the period of instrumental recording (the California Institute of Technology catalog, which runs from 1 January 1932 to 24 September 1986) Appendix I lists the 166 earthquakes with M_L >5.0 that would have caused a peak acceleration at San Diego of greater than 2.0 cm/sec^2 (according to the regression of Joyner and Boore, 1981). Figure 4 shows the epicenters of these events and the most important faults; it brings out two important alignments of earthquakes. The first, and denser, alignment runs along the San Jacinto, Imperial, and Cerro Prieto faults. The second is along the coastal faults and their extension into Baja California - but with a gap at San Diego.

RECORDED STRONG GROUND MOTION

San Diego received its first strong motion accelerograph in 1934, a Coast and Geodetic Survey recorder in the San Diego Light and Power building. There has been only a small increase in the number of accelerographs in San Diego since that time, perhaps because other regions have higher relative hazards. Table 3 lists all the earthquakes known to have triggered any accelerograph in San Diego; Figure 5 shows their epicenters. The series of publications **U. S. Earthquakes** is a reasonably complete source for accelerogram data through 1971. More recent data is fragmented between irregular publications of the U.S. Geological Survey, the California Division of Mines & Geology, and

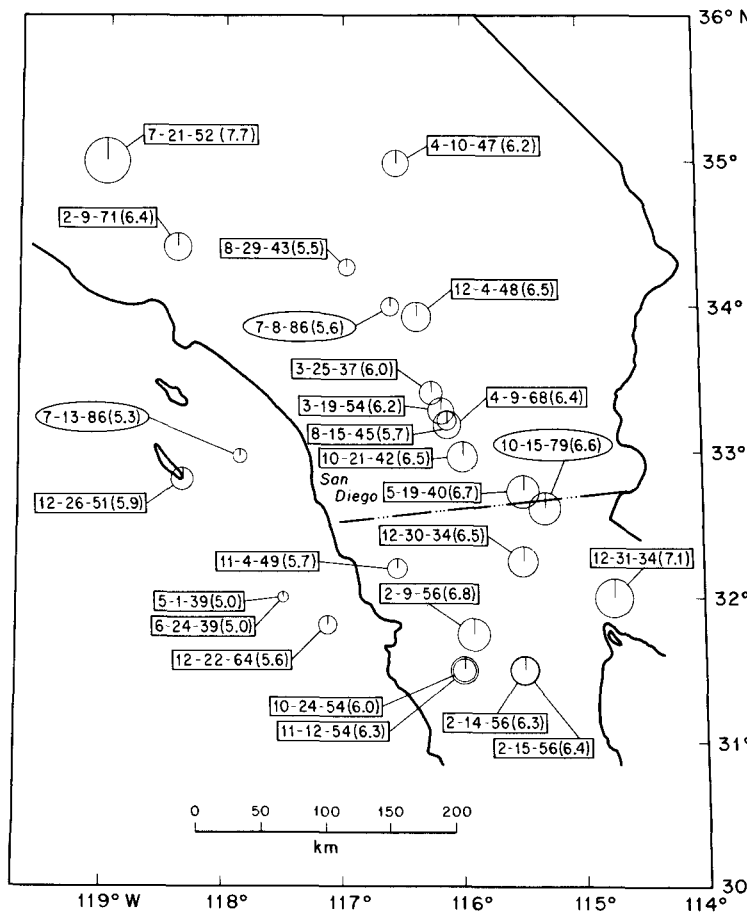

Figure 5 - Epicenters of earthquakes known to have triggered the Coast and Geodetic Survey accelerograph at the San Diego Power and Light building (square boxes) and other accelerographs in San Diego County (elliptical labels) through December 1986.

unpublished sources. In many cases (noted in Table 3) the instrument triggered too late to record the complete S-wave, and thus the records probably missed the actual peak acceleration which occurred during many of the earthquakes. Though peak accelerations are generally small, the high sensitivity (20 mm/0.1 g) of the Coast and Geodetic Survey instrument in San Diego means that the peak values can be reliably estimated.

The greatest peak acceleration recorded at the San Diego Light and Power accelerograph (34 cm/sec^2) was produced by an offshore earthquake on 22 December 1964 (M_L=5.6). That accelerogram triggered during the S-wave, and greater accelerations may have occurred earlier. (Figure 6A). The next strongest ground motions recorded at the San Diego Light and Power building were from earthquakes on the San Jacinto fault zone on 9 April 1968 (M_L=6.8, 29.5 cm/sec^2, Figure 6B) and 21 October 1942 (M_L=6.5, 18 cm/sec^2, Figure 6C). Both of these accelerograms recorded the complete S-wave. All three of these earthquakes caused shaking of intensity VI in San Diego.

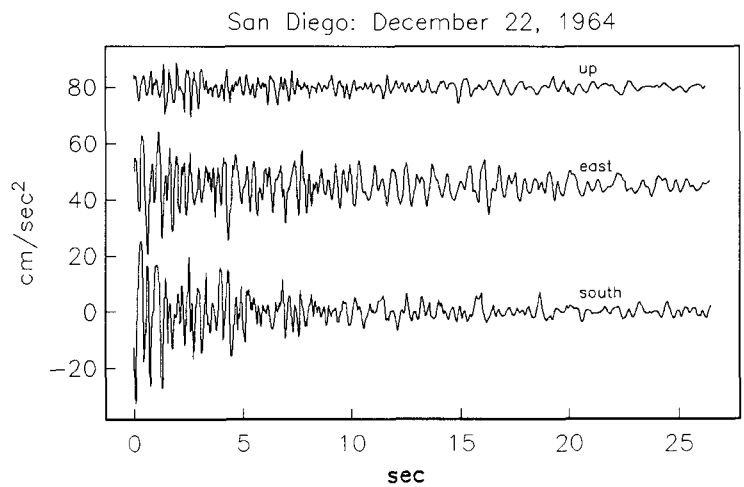

Figure 6a - Accelerograph record from the San Diego Light and Power building from the December 22, 1964 earthquake (Von Hake and Cloud, 1966; quality copy of accelerogram provided by G. Brady, personal communication).

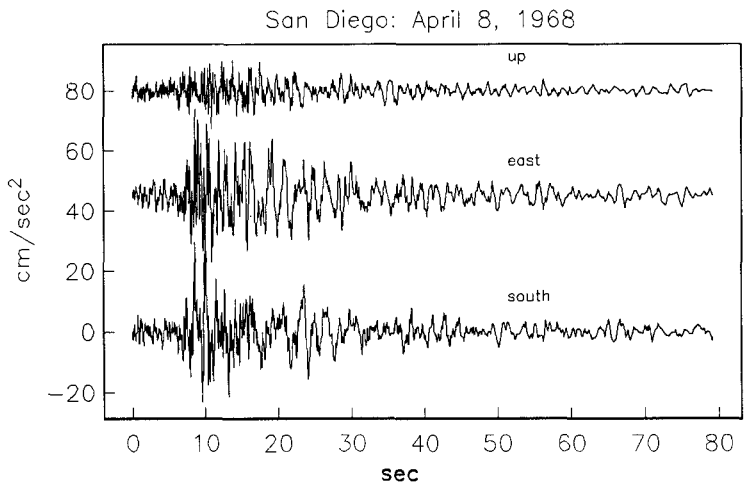

Figure 6b - Accelerograph record from the San Diego Light and Power building for the Borrego Mountain earthquake on April 8, 1968 (EERL, 1971).

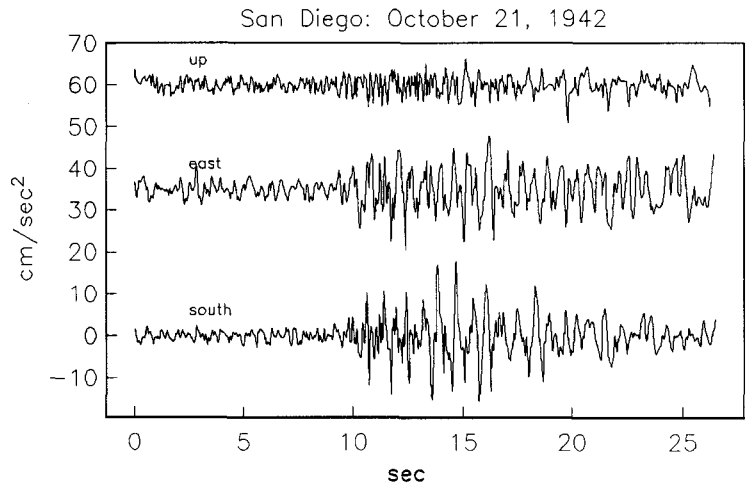

Figure 6c - Accelerograph record from the San Diego Light and Power building from the October 21, 1942 earthquake (Bodle, 1944; quality copy of accelerogram provided by G. Brady, personal communication).

Stronger accelerations were recorded at other stations during three 1986 earthquakes. The July 13, 1986 earthquake (M_L 5.4, with epicenter 50 km west of Solana Beach) gave peaks of about 0.1 g in Ocean Beach and Poway. Since these records were obtained from Kinemetrics SMA-1 accelerographs, with a bandwidth of 0 to 25 Hz, these peak accelerations may have been greater than what would have been recorded on the Coast and Geodetic Survey accelerograph (bandwidth 0 to 12 Hz) for the same ground motion.

Intensity and accelerometer data suggest that San Diego may be in a region of lower attenuation than other parts of California. Figure 7a,b shows isoseismal maps for two earthquakes of similar magnitude, one in the Imperial Valley and the other in the Peninsular Range. The latter has a much larger felt area than the former, suggesting low attenuation in the Peninsular Range. This region is largely comprised of granitic batholithic rock, similar to the Sierra Nevada to the north (though perhaps more fractured by faulting) and with much lower heat flow than the Imperial Valley (Lachenbruch et al., 1985). We should note that while low attenuation in the batholith could explain the data in Figure 7a,b, it may be that earthquakes in the batholith have higher stress drops or some other systematic difference in their source properties. This has not yet been resolved. Figure 7c illustrates this asymmetry in a different way. Geological evidence strongly suggests that the 1892 earthquake occurred on the Southern Elsinore fault (Section 2.3). At this location the fault has a large normal component of slip, and forms the boundary between the Salton trough and the Peninsular Ranges. Figure 7c shows that the isoseismals, taken from Toppozada, are asymmetrical, suggesting much lower attenuation in the Peninsular Ranges toward the west than in the Imperial Valley toward the east.

There is not enough strong motion data recorded at San Diego to prepare a regression appropriate for the region. Thus our approach to evaluate whether the peak recorded accelerations at San Diego are high or low compared to expectations, is to compare them with a regression model that is reasonably representative of the entire California region. For this purpose, the model given by Joyner and Boore (1981) was selected. Table 3 shows the peak value of the larger of the two horizontal components predicted by that model. Among the accelerograms with complete S-waves, the peak accelerations from the San Diego Light and Power station all exceed the regression prediction. Also, one of the records that was triggered late recorded a peak acceleration of 2.7 times the prediction. Among the rest of the records that triggered late, the ratios are near unity or less than one. Although this is consistent with the inference made from the intensity maps in Figure 7a the consequences of possible site effects, if any, are not known.

An exception to the tendency for the regression to underestimate the peak acceleration occurred on the SDG&E Building record of the October 29, 1986 earthquake (M_L=4.7) in National City, where a complete S-wave and most of the P-wave were recorded. The Joyner and Boore regression is extrapolated beyond its formal limits in this case, but still this point is significant because it is at smaller epicentral distances than

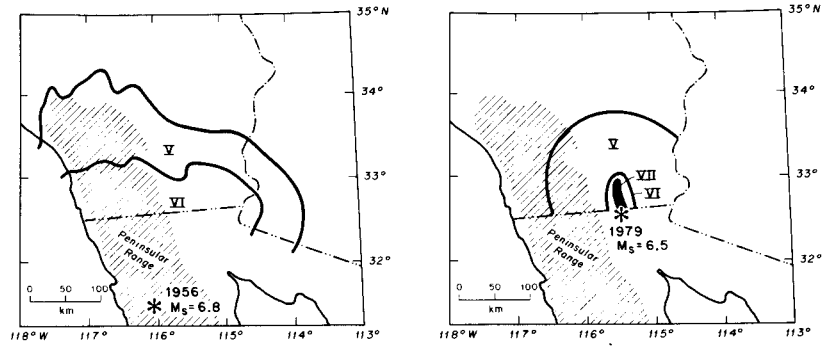

Figure 7a,b - Isoseismals of the 1956 El Alamo earthquake, M_S=6.6 (after Brazee and Cloud, 1958) and of the 1979 Imperial Valley earthquake, M_S=6.5 (after Stover and von Hake, 1981). Shaded area shows the extent of the Peninsular Range consisting primarily of a Cretaceous granite batholith, with less extensive exposures of older sediments and volcanics, metamorphosed by the emplacement of the batholith.

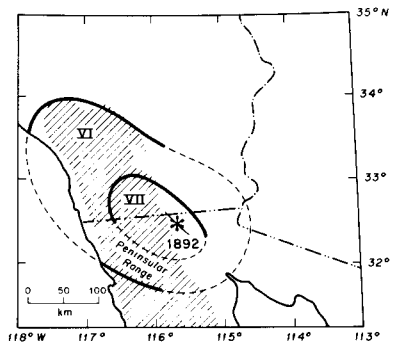

Figure 7c - Isoseismals of the February 23, 1892 southern California earthquake (after Toppozada et al., 1981).

any other record. Thus even if the regression we selected for a reference model systematically underestimates the true peak acceleration in San Diego from more distant earthquakes, it may perform well for nearby events. To summarize, the Modified Mercalli Intensity and strong motion evidence suggests, weakly, that the attenuation is lower in the Peninsular Range batholith, but because of uncertainties in the data more research will be needed to prepare a definitive case.

POSSIBLE FUTURE EARTHQUAKES

The information in the preceding sections could serve as an input to a calculation of the seismic hazard for San Diego. This section attempts to put this information into perspective, but does not complete a seismic hazard analysis. It is limited to consideration of some of the most significant earthquakes that might occur on the major faults in the region.

Table 4

Partial list of plausible earthquakes which could affect San Diego

segment	L km	W km	gam	eff	slip rate (mm/year)	used	rdte	M	R km	A_{max} galyr^{-1}	rate	r.i.
San Andreas												
1 Indio	130.	10.	1.8	1.0	30.0-30.0	30.0	7.0[4]	7.3	140.	19.	.00299	334.
2 Palmdale	175.	12.	1.8	1.0	20.0-35.0	25.0	3.0[4]	7.5	160.	17.	.00095	1050.
2a1 & 2	305.	12.	1.8	1.0	20.0-35.0	25.0	5.0[4]	7.9	140.	26.	.00091	1098.
•3 REPEAT 1857	380.	12.	1.8	1.0	25.0-35.0	35.0	7.0[4]	8.0	180.	18.	.00102	977.
3a1 & 3	580.	12.	1.8	1.0	25.0-35.0	35.0	20.0[4]	8.2	140.	33.	.00192	522.
Cerro Prieto												
•4 1934	100.	10.	1.8	.5	40.0-45.0	40.0	25.0	7.2	160.	14.	.00694	144.
•4aREPEAT 1980	26.	10.	1.8	.5	40.0-45.0	40.0	15.0	6.4	160.	9.	.01603	62.
Imperial												
•5 REPEAT 1940	55.	10.	1.8	.5	30.0-45.0	30.0	15.0	6.8	150.	13.	.00758	132.
•5aREPEAT 1979	40.	10.	1.8	.5	30.0-45.0	30.0	15.0	6.6	150.	12.	.01042	96.
San Jacinto												
6xSupers. H.	26.	10.	1.8	.8	8.0-15.0	12.0	6.0[3]	6.4	125.	14.	.01026	97.
6ySupers. M.	26.	10.	1.8	.8	8.0-15.0	12.0	5.0[3]	6.4	125.	14.	.00855	117.
•7 1968	35.	10.	1.8	1.0	2.8- 5.0	5.0	4.0	6.5	100.	22.	.00635	157.
8 Coyote Mtn	24.	10.	1.8	1.0	2.8- 5.0	5.0	2.5	6.3	100.	20.	.00579	173.
7a6.2 & 7	60.	10.	1.8	1.0	2.8- 5.0	3.0	.5	6.9	100.	26.	.00046	2160.
8a6.2 & 7 & 8	110.	10.	1.8	1.0	2.8- 5.0	5.0	.5	7.2	100.	32.	.00025	3960.
•9 1954	17.	10.	1.8	1.0	6.0-10.0	5.0	2.0	6.1	110.	15.	.00654	153.
10 Clark Valley	40.	12.	1.8	1.0	6.0-10.0	9.0	1.0	6.7	105.	22.	.00139	720.
11 Anza	35.	12.	1.8	1.0	8.0-15.0	12.0	4.0	6.6	105.	21.	.00635	157.
•12 1899	29.	12.	1.8	1.0	4.0- 8.0	6.0	3.0	6.5	110.	18.	.00575	174.
11a10 & 11	75.	12.	1.8	1.0	8.0-15.0	12.0	5.0	7.0	105.	27.	.00370	270.
•12b9 - 12	120.	12.	1.8	1.0	8.0-15.0	12.0	3.0	7.3	105.	32.	.00139	720.
•13 1918	55.	12.	1.8	1.0	4.0-12.0	9.0[2]	3.0	6.9	115.	21.	.00303	330.
•14 1923	30.	12.	1.8	1.0	8.0-15.0	12.0	6.0	6.5	145.	11.	.01111	90.
14a13 & 14	85.	12.	1.8	1.0	4.0- 8.0	6.0	6.0	7.1	115.	24.	.00392	255.
Elsinore - Laguna Salada												
15 Sierra Mayor	49.	10.	8.0	1.0	1.0- 2.0	1.5	1.5	7.2	170.	12.	.00038	2613.
•16 Chupamiertos-1934	22.	10.	8.0	1.0	1.0- 2.0	1.5	1.5	6.7	155.	11.	.00085	1173.
•17 Laguna Salada-1899	38.	10.	8.0	1.0	1.0- 2.0	1.5	1.5	7.0	125.	20.	.00049	2027.
18 Coyote Mtn	60.	10.	2.5	1.0	4.0- 6.0	5.0	5.0	7.0	85.	36.	.00333	300.
19 Julian	80.	12.	1.8	1.0	3.0- 7.0	5.0	2.5	7.1	65.	56.	.00174	576.
20 Temecula	50.	12.	1.8	1.0	3.0- 7.0	5.0	2.5	6.8	70.	44.	.00278	360.
20a19 & 20	130.	12.	1.8	1.0	3.0- 7.0	5.0	2.5	7.4	65.	66.	.00107	936.
•21 Glen Ivy	22.	10.	1.8	1.0	3.0- 7.0	5.0	2.0	6.3	100.	19.	.00505	198.
22 Whittier-Chino	75.	12.	1.8	1.0	3.0- 7.0	5.0	2.0	7.0	120.	22.	.00148	675.
22a21 & 22	95.	12.	1.8	1.0	3.0- 7.0	5.0	3.0	7.2	120.	24.	.00175	570.
San Miguel - Vallecitos												
•23 southern-1956	49.	12.	1.8	1.0	0.5-2.0	1.0	1.0	6.8	160.	11.	.00113	882.
24 central	55.	12.	1.8	1.0	0.5-2.0	1.0	1.0	6.9	105.	24.	.00101	990.
25 northern	75.	12.	1.8	1.0	0.5-2.0	1.0	1.0	7.0	55.	69.	.00074	1350.
Rose Canyon - Newport Inglewood												
26 multiple	50.	12.	1.8	1.0	0.5- 3.0	1.2	.1	6.8	8.	402.	.00011	9000.
26amultiple	18.	12.	1.8	1.0	0.5- 3.0	1.2	1.1	6.2	8.	286.	.00340	295.
27 Mission Bay	24.	12.	1.8	1.0	0.5- 3.0	1.2	.6	6.4	1.	472.	.00139	720.
28 La Nacion	28.	12.	1.8	1.0	.02- .08	.05	.05	6.5	6.	383.	.00010	10080.
29 Del Mar	34.	12.	1.8	1.0	0.5- 3.0	1.2	.6	6.6	22.	154.	.00098	1020.
29a27 & 29	60.	12.	1.8	1.0	0.5- 3.0	1.2	.6	6.9	1.	640.	.00056	1800.
30 Camp Pendleton	70.	12.	1.8	1.0	0.5- 3.0	1.2	1.2	7.0	55.	67.	.00095	1050.
•31 1933	37.	12.	1.8	1.0	0.5- 3.0	1.2	1.2	6.6	125.	16.	.00180	555.
Agua Blanca - Coronado Banks												
32 Valle Trinidad	65.	12.	1.8	1.0	4.0- 6.0	6.0	6.0	7.0	175.	10.	.00513	195.
33 Santo Tomas	32.	12.	1.8	1.0	4.0- 6.0	6.0	6.0	6.5	150.	11.	.01042	96.
34 Punta Banda Rdg	29.	12.	1.8	1.0	4.0- 5.0	4.0	4.0	6.5	125.	15.	.00766	130.
35 multiple	>250.	12.	1.8	1.0	2.0- 6.0	3.0	.01	7.7	26.	250.	.00000	
35amultiple	>85.	12.	1.8	1.0	2.0- 6.0	3.0	1.5	7.1	26.	175.	.00098	1020.
35bmultiple	>15.	12.	1.8	1.0	2.0- 6.0	3.0	1.5	6.1	26.	98.	.00556	180.
San Diego Trough												
36 multiple	>250.	12.	1.8	1.0	0.05- 1.0	1.0	.01	7.7	41.	149.	.00000	
36amultiple	>85.	12.	1.8	1.0	0.05- 1.0	1.0	.5	7.1	41.	104.	.00033	3060.
36bmultiple	>15.	12.	1.8	1.0	0.05- 1.0	1.0	.5	6.1	41.	58.	.00185	540.

Table 4 (cont.)

San Clemente - San Isidro												
37 multiple	>250.	12.	1.8	1.0	0.5- 5.0	5.0	.01	7.7	80.	61.	.00000	
37amultiple	>200.	12.	1.8	1.0	0.5- 5.0	5.0	2.5	7.6	80.	57.	.00069	1440.
37bmultiple-12/26/51(5.9)	>35.	12.	1.8	1.0	0.5- 5.0	5.0	2.5	6.6	80.	32.	.00397	252.
Transverse Ranges thrust system												
38 multiple	>250.	12.	8.0	1.0	1.0-10.0	5.0	.01	8.2	165.	23.	.00000	
38amultiple	>30.	12.	8.0	1.0	1.0-10.0	5.0	5.0	6.9	165.	12.	.00208	480.

Notes:

event = a plausible earthquake which would occur as the result of failure of some particular fault segment which is identified in this column.

L = length of fault segment, or combination of segments. Note, for segments which are identified as "multiple", this column gives the total fault length. Rounding: nearest 5 km for L>50 nearest 1 km for L<50

W = Assumed width of fault segment rupture.

gam = Assumed ratio of slip to fault length, $\times 10.0^5$

eff = fraction of slip that occurs in earthquakes - rest is creep

slip rate = reasonable range of slip rate obtained from geological data, as discussed in the text.

used = slip rate that we use for this segment of the fault.

rdte = rate distributed to earthquakes. When more than one size earthquake is allowed to occur on a single fault segment, then we presume that each size event must take up a certain portion the total slip rate. This column gives the portion assumed for the event of this size. The sum of the columns under "rdte" for any fault segment must sum to the rate "used".

M = magnitude of hypothesized event. This magnitude is the moment magnitude of an earthquake which ruptures the fault segment length with a fault width and ratio of slip to length "gam" as given. For faults segments which are identified as "multiple", we estimate the magnitude of the largest event we consider plausible on the fault; this magnitude is not derived from the fault length. For segments identified as multiple, we also identify the magnitude of a more probable earthquake size, and distribute most of the slip to that size.

R = Distance from closest point on the fault segment to downtown San Diego.
Rounding: nearest 5 km for L>50
nearest 1 km for L<50

A_{max} = peak acceleration as estimated from the Joyner & Boore (1981) regression.

rate = average occurrence rate of events with the magnitude given. The rate is consistent with slip rate constraints (e.g., Anderson, 1979, Anderson & Luco, 1983) on all fault segments, including segments on which more than one plausible earthquake magnitude has been hypothesized. (Rounded to two significant figures.)

years = average recurrence time of event with the given magnitude. This time is 1/rate.

Footnotes:

• Historical earthquake

1 In the historical record, Anderson & Bodin (1987) found that over two earthquake cycles there is significant aseismic slip relative to these hypotheses.

2 This rate averages 6 mm/yr in the southern half where zone 12 overlaps and 12 mm/yr in the northern half of the segment.

3 Division of slip between these two faults arbitrary.

4 Division of slip among differing sizes of events results in occurrence rates consistent with historical data.

Table 4 lists these discrete events, based on the segmentation of the faults given in Table 1. For each fault segment we have estimated a plausible magnitude for the earthquake consistent with the rupture length and a plausible occurrence rate for the earthquake consistent with the fault slip rate. Smaller earthquakes (M<6) can occur on any of these faults and generally do not affect the rate of the large events considered here.

The magnitude-rupture length relationship employed is based on the definition of seismic moment and the observation by Scholz (1982) that the ratio of slip to fault length, γ, appears to be about constant. With this assumption, the rupture length, L, is given by

$$L=L_o\ 10^{(d/2)M}$$

where

$$L_o = [10^c/(\mu\gamma\ W)]^{1/2} \quad \text{(Anderson \& Luco,1983).}$$

In this expression, μ is the shear modulus, W is fault width, and the relationship between magnitude and seismic moment is $\log M_0 = c+dM$. We use c=16.0, d=1.5, $\mu = 3 \times 10^{11}$ dyne-cm^{-2}, and W = 10 km for faults in the Salton trough or W = 12 km for faults elsewhere. Scholz (1982) recognized that the value of γ varies with the nature of slip on the fault; it also depends on the fault slip rates (Kanamori & Allen, 1986). The values of γ used here (Table 4) are consequently greater for normal or thrust faults than for strike slip, and for the strike slip faults, γ is slightly greater than the value suggested by Scholz (1982) because most of the faults have low slip rates. Table 5 validates this relationship.

Different techniques were employed to obtain earthquake occurrence rates in Table 4 consistent with fault slip rate. For typical cases (e.g., segments 6-9, 12-18, etc.) we have a single fault segment, on which we estimate a "characteristic" magnitude from the segment length. Based on the Scholz (1982) hypothesis, again, that the ratio of average slip to fault length is constant, we obtain an estimate of the slip per event. The occurrence rate is fault slip rate divided by slip per event, assuming the entire fault slip rate is released seismically (Wallace, 1970).

Adjacent segments sometimes rupture together to produce larger earthquakes, as seen in the historical or prehistorical records from the San Andreas, Imperial, and Cerro Prieto faults. It is necessary to include this in our model, for otherwise many segments yield recurrence rates that are inconsistent with the seismic history since 1800 or as revealed in the geology. There is some flexibility associated with the combination of multiple segments, which we have used as a tool to achieve the maximum consistency with the geological record. When multiple ruptures on the same segment are allowed, some technique is needed to decide the relative occurrence rates of the smaller and larger earthquakes. A simple b-value model appears to be inconsistent with observa-

Table 5

Comparison of predicted and observed magnitudes for several earthquakes within the study region.

Segment	Earthquake year	L	Magnitude calculated from L	Magnitude historical[1]
3	1857	380	8.0	7.9[2]
4a	1980	26	6.4	6.4[3]
5	1940	55	6.8	7.0[3]
7	1968	35	6.5	6.4
9	1954	17	6.1	6.2
12	1899	29	6.5	6.6[7]
13	1918	55	6.9	6.8
14	1923	30	6.5	6.25
16	1934	22	6.7	6.5
17	1892	38	7.0	6.9
21	1910	22	6.3	6.3[5]
23	1956	49	6.8	6.8
31	1933	37	6.6	6.3
18	prehistoric	60	7.0	6.9–7.0[6]

Notes:

1 M_W when footnote gives source, M_L otherwise.

2 Sieh (1978b)

3 Anderson & Bodin (1987)

4 Based on geological evidence for 5 m slip over 22 km rupture length (Mueller & Rockwell, 1984, 1987 in press)

5 Based on geological evidence for 35 cm slip at Glen Ivy, assumed 22 km rupture length (Brake & Rockwell, 1987; Brake 1987)

6 Based on geological evidence for 1.5 m slip over at least 45 km rupture length (Jacoby et al., 1986)

7 Toppozada et al. (1981)

tions (e.g., Bath, M., 1981; Singh et al., 1982; Schwartz and Coppersmith, 1984; Wesnousky, 1986; Anderson & Bodin, 1987). With this recognition, the shape of the distribution of large magnitude events for a single fault is poorly constrained. Therefore, rather than use a continuous and smooth distribution function as in Anderson (1979), Molnar (1979), Youngs and Coppersmith (1985) or Anderson and Bodin (1987), we partitioned the slip to selected discrete events. The slip rate caused by the selected event type is given in the "rdte" column of Table 4. A simple example occurs on segments 21 and 22 of the Elsinore-Laguna Salada fault system. Small events, such as the 1910 earthquake, evidently occur on segment 21, but the geological record supports a longer recurrence time than what would occur if the entire 5 mm/yr occurs in events with only 350 mm slip. The geological evidence also suggests that some of the events on this segment have more than 350 mm slip. We assumed that small events involving only segment 22 contribute 2 mm/yr to the fault slip, and that events involving both segments 22 and 23 contribute the remaining 3 mm/yr. Even in more complicated cases, such as on the San Andreas fault, we found that we could

similarly divide the slip more or less evenly among the different plausible events and obtain reasonably good consistency with the geological constraints.

Offshore faults were treated under these same rules, except that the sizes of earthquakes were taken as extreme for the larger events suggested for a fault segment and typical for the smaller segment. Finally, we adjusted the rates for aseismic slip, such as is observed on the Imperial and Cerro Prieto faults (Anderson & Bodin, 1987).

Each of the earthquakes from Table 4 has been plotted in Figure 8. The most significant possible events are those which have a combination of a high occurrence rate and a high peak ground acceleration. Specific events on Table 4 that meet these criteria are on the Rose Canyon fault, the Coronado Banks fault, the San Diego Trough fault, and the Elsinore fault. At higher probabilities and lower levels of ground motion, the San Jacinto fault is most important, exceeding the San Andreas, Cerro Prieto, Imperial, and onshore faults in Baja California.

Table 4 is by no means a complete enumeration of all possible earthquakes, but we expect that it is reasonably complete for the major earthquakes on major faults. Therefore, we used these data to obtain a cumulative curve (based on Figure 8) for the probability of ground motion equaling or exceeding the abscissa value from the events considered in our model. The result is in the style of a probabilistic seismic hazard analysis, but differs significantly. A complete probabilistic seismic hazard analysis would include a consideration of the uncertainty in ground motion estimates, and a distribution of magnitude for each fault, in effect "smearing out" each of the points on Figure 8. The addition of smaller events would shift the cumulative curve upwards. The complete analysis would also consider multiple models for activity rates on faults and for attenuation, rather than the single models that we employed. Power et al. (1986) have carried out such an analysis. Our cumulative curve gives higher accelerations than Power et al. at occurrence rates less than 10^{-2} yr^{-1} but the studies are consistent at higher occurrence rates; the difference arises from higher assumed slip rates on the Rose Canyon fault zone in our study.

The solid lines on Figure 8 give an estimate of the historical rate of exceedance of weaker ground motions for San Diego, following the historical method of Milne and Davenport (1969). The analysis proceeded in the following manner. We estimated the peak accelerations, again using the regression of Joyner and Boore (1981), based on the magnitude and distance to San Diego for each of the N earthquakes (with magnitude exceeding a threshold) in the catalog. These peak values were then sorted in increasing order. The largest acceleration then was equalled or exceeded at a rate of 1/Y where Y is the duration of the catalog, and in general, the i-th largest acceleration was equalled or exceeded at a rate of i/Y, so that each peak acceleration was associated with a corresponding number of exceedances per year. Figure 8 shows the result for a catalog that includes earthquakes with $M_L >= 6.0$ (Appendix I). Smaller events were excluded because none of the earthquakes listed in

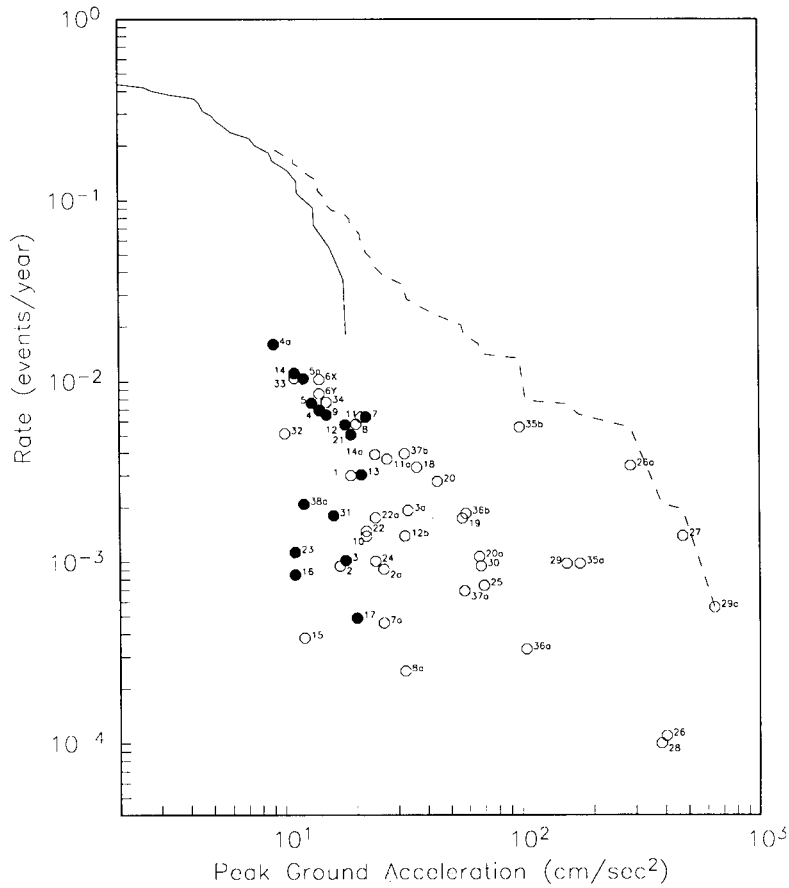

Figure 8 - This figure shows two types of information. The numbered data points represent specific hypothesized events, as given in Table 4 and Figure 2. The dashed line is the cumulative expected rate of exceedance of peak acceleration obtained from the numbered events. Solid symbols are events that have occurred once or more in historical times. The solid lines show the historical occurrences of peak acceleration as a function of mean annual occurrence rate, January 1, 1932 to September 24, 1986, based on historical method. For consistency, all accelerations are based on the regression of Joyner and Boore (1981). This result differs from a complete seismic hazard analysis because small events and minor faults are not considered. Events with magnitude between 5 and 6, and possibly some events with magnitude over 6, are not represented because of the way this figure was generated. Such events would increase the occurrence rate of all accelerations and are quite significant for the total seismic hazard.

Table 4 are smaller than that. Similar analyses for smaller events increase the peak acceleration at any given rate of exceedances per year (i.e., the solid line shifted to the right). The cumulative curve obtained from Table 4 is consistent with the range of occurrence rates from this historical method for peak accelerations in the vicinity of 10 to 20 cm/sec^2.

Similarly, a historical curve can be generated from the table of peaks recorded on strong motion accelerographs; the result is reasonably consistent with the historical curve from the earthquake catalog, but the completeness is uncertain. If we adopt a relationship between intensity and peak acceleration, the pre-instrumental history can also be adapted to the format in Figure 8, and appears to be consistent for occurrence rates above about 5×10^{-3} yr^{-1}. From these consistency checks, we conclude that the geological model in Table 4 is not seriously biased at these higher occurrence rates.

Some of the discrete events on Figure 8 have already occurred. These are indicated by a solid symbol. About half of the plausible earthquakes with recurrence times of greater than 250 years have already occurred; this proportion is about right. None of the low-probability earthquakes with expected accelerations over 30 cm/sec^2 have occurred, even though some of the low probability events that give lower accelerations are represented in the historical record. The larger accelerations come from the Rose canyon, Elsinore and offshore fault zones, all of which have been inactive during historical time. Not enough is known about the behavior of offshore faults to have much confidence in our models for their behavior. Additional geological studies of the onshore faults are also likely to lead to revisions in Table 4, but we are confident that many of those events are plausible and will eventually happen.

Many of the discrete events from Table 4 could be expected to cause ground motions comparable to, or greater than, the ground motions associated with the magnitude 5.3 earthquake which occurred offshore of Solana Beach on 13 July, 1986, which injured twenty-nine people and caused damage to at least 50 buildings in the Newport Beach - San Diego area. A preliminary estimate of damage in the U.S. was 720,000 dollars; some damage was also reported in the Tijuana area (PDE, Monthly listing, July 1986, USGS).

The possible effect of a major earthquake, as currently anticipated on the San Andreas fault, can perhaps be envisioned from the effects of the 8 July 1986 North Palm Springs earthquake. The North Palm Springs earthquake occurred on the San Andreas fault, and thus might be regarded as a Green's function for the ground motion from a great earthquake there. This earthquake had an aftershock zone about 15 km long (Nicholson et al., 1986), while the eventual great earthquake might have a rupture length of about 150 to 200 km, implying that the duration for the larger earthquake would be about 10 times greater. For a magnitude difference of 2.2 magnitude units (7.9-5.7), the Joyner and Boore regressions predicts peak accelerations which are increased by a factor of three to four times, and peak velocities increased by a factor of 10

to 15. At 140 km distance, Joyner and Boore (1981) predict peak accelerations increasing from 7 cm/sec^2 for magnitude 5.6 to 27 cm/sec^2 for magnitude 7.9. However, in the July 8 earthquake (M=5.6) the peak acceleration at Murray Dam, 12 km east of downtown San Diego, was already about 30 cm/sec^2; if the ratio from the Joyner and Boore regression holds, the peak acceleration in San Diego could be as high as 150 cm/sec^2 in a large earthquake on the San Andreas fault. According to Trifunac and Brady (1975) this level of shaking could correspond to intensity VII to VIII, which is surprising when we consider that the 1857 earthquake only caused intensity V. The Indio segment is closer to San Diego, and particularly closer than the Carrizo Plains which was the part of the San Andreas with most slip in 1857, so it appears that San Diego should expect a higher intensity than in the 1857 earthquake. Thus San Diegans would be wrong to assume that they are far enough from the San Andreas fault to be isolated from damaging ground motions.

SUMMARY

This paper identifies the major faults which contribute to the seismic hazard for San Diego, compiles estimates of their activity rates, examines the attenuation of ground motion in the area, and combines this information to estimate the seismic hazard. We point out here, again, major uncertainties, and directions of future research which will be needed to reduce these uncertainties. From the geological viewpoint, the greatest uncertainty is in the slip rates of the Rose Canyon and offshore faults, and the size and recurrence rates of earthquakes that these faults produce. For each of the faults, we suggest possible segments which might tend to break coherently in single earthquakes. Future earthquakes will test this preliminary model, and additional research also is certain to result in more detailed knowledge about the geometrical characteristics and modes of rupture of the southern California faults which will require revisions to the model.

The attenuation model for ground motion near San Diego needs to be reconsidered carefully, as some evidence suggests that the area may be in a low attenuation region compared to other locations in California which have produced strong motion data. This problem can be studied in part with recordings of small earthquakes; it is not necessary to wait for large ones. An urban seismic network would also allow a quantitative study of local site effects, which are certain to cause variations in the ground motion from one locality to another within the urban area.

The model of significant earthquakes to San Diego which we present has not been developed to the point where the effects of the various uncertainties are presented. Methods are available to handle all of the uncertainties discussed above, and they ought to be applied to improve upon our results, but that analysis is beyond the scope of this research.

In spite of the uncertainties, we believe that the model given by this paper captures the most significant elements of the seismic hazard

for the San Diego region. In this model, strong earthquakes are expected to occur infrequently in locations close to the metropolitan region. Damage might also occur from more frequent events at greater distances, including the southern San Andreas fault.

ACKNOWLEDGEMENTS

We thank A.G. Brady at USGS for supplying copies of most of the accelerograms that have been recorded at the San Diego Light and Power station. We thank Roger Sherburne at CDMG for copies of accelerograms gathered by the California Division of Mines & Geology Strong Motion Instrumentation Program, and the Institute of Geophysics & Planetary Physics for partial salary support for one of the authors (JGA).

AUTHOR'S NOTE

After the preparation of the bulk of this manuscript, three major earthquakes occurred in southern California. The Whittier Narrows earthquake, Oct. 1, 1987 (M_L 5.9), had a thrust mechanism at a depth of 15 km. Thus it appears to be a small event associated with the southern margin of the Transverse Ranges (ie. smaller than event 38a, Table 4), with its hypocenter located below the north end of the mapped location of the Whittier fault. The first large earthquake in the Superstition Hills sequence, M_S=6.2, Nov. 23, 1987 (PST), ruptured a northeast trending left-lateral fault (the Almore Ranch fault), previously unrecognized as a seismogenic fault. The Nov. 24 M_S=6.6 earthquake ruptured segment 6 on Fig. 2. The magnitude was slightly larger than the anticipated magnitude of 6.4 (Table 4).

REFERENCES

Agnew, D. C. and K. E. Sieh (1978). A documentary study of the felt effects of the great California earthquake of 1857. Bull. Seism. Soc. Am. 68, 1717-1729.

Agnew, D. C., M. Legg and C. Strand (1979). Earthquake history of San Diego, in Abbot, P. and W. Elliott (eds.), Earthquakes and Other Perils: San Diego Region, San Diego Association of Geologists, San Diego, Calif. 123-128.

Anderson, J.G. (1979). Estimating the seismicity from geological structure for seismic risk studies, Bull. Seism. Soc. Am.,69, 135-158.

Anderson, J. G. (1983). Synthesis of seismicity and geological data in Southern California, U.S. Geological Survey Final Technical Report 14-08-0001-G949.

Anderson, J. G. (1984). Synthesis of seismicity and geological data in California, U.S. Geological Survey Open File Report 84-424, Denver, CO.

Anderson J.G. and P. Bodin (1987). Earthquake recurrence models and historical seismicity in the Mexicali-Imperial Valley, Bull. Seism. Soc. Am. 77, 562-578.

Anderson, J.G. and J.E. Luco (1983). Consequences of slip rate constraints on earthquake occurrence relations, Bull. Seism. Soc. Am., 73, 471-496.

Bath, M. (1981). Earthquake recurrence of a particular type, PureAppl. Geophys. 119, 1063-1076.

Bodle, R.R. (1944) U. S. Earthquakes 1942, U.S. Department of Commerce Coast and Geodetic Survey, Washington.

Brake, J.F. (1987). Analysis of historic and prehistoric slip on the Elsinore fault at Glen Ivy Marsh, Temescal Valley, Southern California, unpublished Masers Thesis, San Diego State University, 107 pages.

Brake, J.F. and Rockwell, T. K. (1987). Magnitude of slip from historical and prehistorical earthquakes on the Elsinore fault, Glen Ivy March, southern California (abstract), Geol. Soc. Amer. Abstract with Programs 19, No. 6, page insert.

Brazee, R.J. and W.K. Cloud (1958). United States Earthquakes 1956, U.S. Department of Commerce Coast and Geodetic Survey, Washington.

Campbell, K.W. (1981). Near-source attenuation of peak horizontal acceleration, Bull. Seism. Soc. Am. 71, 2039-2070.

Clark, M. (1972). Surface rupture along the Coyote Creek fault, U.S. Geological Survey Professional Paper 787, 55-86.

DeMets, C., R. G. Gordon, S. Stein, and D. F. Argus (1987). A revised estimate of Pacific-North America motion and implications for western North America plate boundary zone tectonics, Geophys. Res. Letters 14, 911-914.

EERL (1971). Strong motion earthquake accelerograms, digitized & plotted data, V. II - Corrected accelerograms & integrated ground velocity & displacement curves, Part A - accelerograms IIA001 through IIA020, EERL 71-50, Earthquake Engineering Research Laboratory, Calif. Inst. of Technology, Pasadena, Calif., 321 pp.

Feragan, E. S. (1986). Geology of the southeastern San Felipe Hills, Imperial Valley, California: with emphasis on the geometry of structural fabrics in the Borrego formation, Master's Thesis, San Diego State University, 144pp.

Green, H. G., K. A. Bailey, S. H. Clarke, J. I. Ziony, and M. P. Kennedy (1979). Implications of fault patterns of the inner California Continental Borderland between San Pedro and San Diego: in Abbott, P.L. and W. J. Elliott (eds.), Earthquakes and Other Perils, San Diego Region, San Diego Association of Geologists, 21-29.

Harvey, T. W. (1986). Geology of the San Miguel fault zone, Northern Baja California, Mexico (abstracts), Geol. Soc. Amer. Abstracts with programs, Cordilleran Section, Los Angeles, Calif.

Hatch, M.E. (1987). Neotectonics of the Agua Blanca fault, Valle Agua Blanca, Baja California, Mexico, Unpublished Masters Thesis, San Diego State University, San Diego, Calif.

Herzog, L. A., ed. (1986). Planning the international border metropolis: Trans-boundary policy options in the San Diego-Tijuana region, Monograph Series 19, Center for U.S.-Mexican Studies, UC San Diego, La Jolla, CA, p. 63.

Jacoby, G. C., P. R. Sheppard, and K. E. Sieh (1987). Was the 8 December 1812 California earthquake produced by the San Andreas fault? Evidence from trees near Wrightwood, Bull. Seism. Soc. Amer. (in press).

Joyner, W.B. and D.M. Boore (1981). Peak horizontal acceleration and velocity from strong-motion records including records from the 1979 Imperial Valley, California, earthquake, Bull Seism. Soc. Am. 71, 2011-2038.

Kanamori, H. and C. R. Allen (1986). Earthquake repeat time and average stress drop, in S. Das, J. Boatwright, and C. H. Scholz, eds., Earthquake Source Mechanics, Geophys. Monog. 37, 227-235, Amer. Geophys. Union, Washington, D.C.

Kennedy, M. P. (1975). Geology of the San Diego metropolitan area, California, CDMG Bulletin 200, 56pp, Sacramento, Calif.

Kennedy, M.P. and E. E. Welday (1980). Recency and character of faulting offshore metropolitan San Diego, California, Calif. Division of Mines & Geology, Map Sheet 40.

King, N. E. and J. C. Savage (1983). Strain-rate profile across the Elsinore, San Jacinto, and San Andreas faults near Palm Springs, California, 1973-81, Geophys. Res. Letters 10, 55-57.

Lachenbruch, A. H., J. H. Sass, and S. P. Galanis (1985). Heat flow in southernmost California and the origin of the Salton Trough, J. Geophys. Res. 90, 6709-6736.

Lamar, D.L. and T. K. Rockwell (1986). An overview of the tectonics of the Elsinore fault zone, in, Ehlig, P. (ed.) Guidebook and Volume on Neotectonics and Faulting in Southern California, Cordilleran Section, Geol. Soc. of Amer., 149-158.

Legg, M. and D. C. Agnew (1979). The 1862 earthquake in San Diego in San Diego, in Abbot, P. and W. Elliott (eds.), Earthquakes and Other Perils: San Diego Region: 139-141, San Diego Association of Geologists, San Diego, Calif.

Legg, M.R. and M. P. Kennedy (1979). Faulting offshore San Diego and Northern Baja California, in Abbot, P. L. (ed.), Earthquakes and Other Perils: San Diego Region: Geol Soc. Am. Field Trip Guidebook, San Diego Assoc. of Geologists, Nov. 1979.

Legg, M. R. (1985). Geological structure and tectonics of the inner continental borderland offshore Northern Baja California Mexico, Unpublished Ph.D. Thesis, University of California, Santa Barbara.

Leeds, A. L. (1979). Relocation of m > 5.0 Northern Baja California earthquakes using S-P Times, unpublished M.S. thesis, University of California, San Diego, 101 pages.

Millman, D.E. and T. K. Rockwell (1986). Neotectonics of the Elsinore fault in Temescal Valley, California: in Ehlig, P. (ed.) Guidebook and Volume on Neotectonics & Faulting in Southern California, Cordilleran Section, Geol. Soc. Amer., 159-166.

Milne, W. G. and A. G. Davenport (1969). Distribution of earthquake risk in Canada, Bull. Seism. Soc. Am. 59, 729-754.

Molnar, P. (1979). Earthquake recurrence intervals and plate tectonics, Bull. Seism. Soc. Am. 69, 115-133.

Mueller, K. J. (1984). Neotectonics, alluvial history and soil chronology of the southwestern margin of the Sierra de los Cucapas, Baja California Norte, unpublished M.S. Thesis, San Diego, State University, Calif., 363pp.

Mueller, K. J. and T. K. Rockwell (1984). Basin development and fault kinematics of the Laguna Salada rhombochasm, Baja California Norte, Geol. Soc. Am., Abstracts with programs 16, No. 6, p. 624.

Nicholson, C. R. L. Wesson, D. Given, J. Boatwright, and C. R. Allen (1986). Aftershocks of the 1986 North Palm Springs earthquake and relocation of the 1948 Desert Hot Springs earthquake, (Abstract), EOS, Trans. AGU 67, Nov. 4, 1986 1089.

Pinault, C.T. and Rockwell (1984). Rates and sense of Holocene faulting on the southern Elsinore fault: further constraints on the distribution of dextral shear between the Pacific and North American plates. GSA Abstracts with programs vol 16, no 6, p624.

Power, M. S., V. Berger, R. R. Youngs, K. J. Coppersmith, and D. W. Streiff (1986). Evaluation of liquefaction opportunity and liquefaction potential in the San Diego, California urban area, Final Technical Report 14-08-0001-20607, U.S. Geological Survey, 90pp + figures.

Reichle, M., P. Bodin, and J. Brune (1985). The June 1985 San Diego Earthquake Swarm, (Abstract), EOS Transactions, American Geophysical Union 66, 952.

Reyes, A. and Lopez, A. (1985). Prediccion de la distribucion del movimiento fuerte del terreno en el valle Imperial-Mexicali para dos terremotos de magnitud postulada M=7.0 y 7.4, in Riesgo Sismico En La Baja California, Memoirs of the Sociedad Mexicana de Mecanica de Suelos, A.C., Mexicali, Baja California, Mexico, May 1985, 15-40.

Rockwell, T. K., R. S. McElwain, D. E. Millman, and D. L. Lamar (1986). Recurrent late Holocene faulting on the Glen Ivy North strand of the Elsinore fault at Glen Ivy Marsh, in Ehlig, P. (ed.) Guidebook and Volume on Neotectonics & Faulting in Southern California, Cordilleran Section, Geol. Soc. Amer., 167-175.

Rockwell, T. K. M. E. Hatch, and D. L. Schug (1987). Late Quaternary rates: Agua Blanca and borderland faults, Final Technical Report, U. S. Geological Survey, 122 pp.

Rockwell, T.K., and Pinault, C.T. (1986). Holocene slip events on the southern Elsinore fault, Coyote Mountains, southern California. in Guidebook and Volume on Neotectonics and Faulting in Southern California, Cordilleran Section, Geol Soc. Amer., 193-196.

Rockwell, T.K., Loughman, C., and Merifield, T., (1988). Late Quaternary rate of slip along the San Jacinto fault zone near Anza, southern California, submitted to JGR, May 1988.

Sanders, C.O. and H. Kanamori (1984). A seismotectonic analysis of the Anza seismic gap, San Jacinto fault zone, southern California, J. Geophys. Res. 89:B7, 5873-5890.

Sanders, C.O., H. Magistrale, and H. Kanamori (1986). Rupture patterns and preshocks of large earthquakes in the Southern San Jacinto fault zone, Bull. Seism. Soc. Am. 76, 1173-1187.

Scholz, C. H. (1982). Scaling laws for large earthquakes, consequences for physical models, Bull. Seism. Soc. Am. 72, 1-14.

Schug, D. L. (1987). Neotectonics of the western reaches of the Agua Blanca fault, Baja California, unpublished masters thesis, San Diego State University, San Diego, California, 128 pp.

Schwartz and K. Coppersmith (1984). Fault behavior and characteristic earthquakes: examples from the Wasatch and San Andreas fault zones, J. Geophys. Res. 89, 5681-5698.

Schwartz, D.P. and K. J. Coppersmith (1986). Seismic hazards: new trends in analysis using geologic data, in Active Tectonics, National Academy Press, Washington D.C. 215-230.

Sharp, R. V. (1981). Variable rates of late Quaternary strike-slip on the San Jacinto fault zone, southern California, J. Geophys. Res. 86, 1754-1762.

Shor, G. G. Jr., and E. Roberts (1958). San Miguel, Baja California Norte earthquakes of 1956: A field report, Bull. Seism. Soc. Am. 48, 101-116.

Sieh, K. (1978a). Pre-historic large earthquakes produced by slip on the San Andreas fault at Pallett Creek, California, J. Geophys. Res., 83 3907-3939.

Sieh, K. (1978b). Slip along the San Andreas fault associated with the great 1857 earthquakes, Bull. Seism. Soc. Am. 68, 1421-1428.

Sieh, K. (1984). Lateral offsets and revised dates of large earthquakes at Pallett Creek, California, J. Geophys. Res. 89, 7641-7670.

Sieh, K. (1986). Slip rate across the San Andreas fault and prehistoric earthquakes in Indio, California (Abstract), EOS Trans. Am. Geophys. Union, 67, 1200.

Sieh, K. and R. E. Jahns (1984). Holocene activity of the San Andreas fault at Wallace Creek, California, Geol. Soc. Amer. Bull. 95, 883-896.

Simons, R.S. (1977). Seismicity of San Diego, 1934-1974, Bull Seism. Soc. Am. 67, 809-826.

Singh, S.K., R. J. Apsel, J. Fried, and J. N. Brune (1982). Spectral attenuation of SH-waves along the Imperial fault, Bull. Seism. Soc. Am. 72, 2003-2016.

Stover, C.W. and C.A. vonHake (1981). United States Earthquakes, 1979, U.S. Department of the Interior Geological Survey and U.S. Department of Commerce National Oceanic and Atmospheric Administration, Golden, Colorado.

Strand, C. L. (1980). Pre-1900 earthquakes of Baja California and San Diego County, M.S. Thesis, San Diego, State University, San Diego, CA.

Sykes, L. R. and S. P. Nishenko (1984). Probabilities of occurrence of large plate rupturing earthquakes for the San Andreas, San Jacinto, and Imperial Faults, California, 1983-2003.

Thatcher, W. (1983). Nonlinear strain buildup and the earthquake cycle on the San Andreas fault, J. Geophys. Res. 88, 5893-5902.

Toppozada, T.R., D.L. Parke, and C. Real (1981). Preparation of isoseismal maps and summaries of reported effects for pre-1900 California earthquakes, California Division of Mines and Geology Open File Report 81-11, Sacrament, CA.

Toppozada, T.R., and D.L. Parke (1982). Areas damaged by California earthquakes 1900-1949, California Division of Mines and Geology Open-File Report 82-17, Sacramento, CA, 65 pp.

Vaughn, P.R. (1987). Alluvial stratigraphy and neotectonics along the Elsinore fault at Agua Tibia mountain, California, unpublished Masters thesis, University of Colorado, Boulder, 182 pages.

Vaughan, P. and T. Rockwell (1986). Alluvial stratigraphy and neotectonics of the Elsinore fault zone at Agua Tibia Mountain, southern California, in Ehlig, P. (ed.) Guidebook and Volume on Neotectonics & Faulting in Southern California, Cordilleran Section, Geol. Soc. Amer., 177-191.

Von Hake, C. A. and W.K. Cloud (1966). United States Earthquakes 1964, U.S. Department of Commerce Coast and Geodetic Survey, Washington.

Wallace, R. E. (1970). Earthquake recurrence intervals on the San Andreas fault, Bull. Geol. Soc. Am. 81, 2875-2890.

Weldon, R. and K. Sieh (1985). Holocene rate of slip and tentative recurrence interval for large earthquakes on the San Andreas fault, Cajon Pass, southern California, Geol. Soc. Amer. Bull. 96, 793-812.

Wells, D. L. (1987). Geology of the eastern San Felipe Hills, Imperial Valley, California: Implications for wrench faulting in the southern San Jacinto fault zone, unpublished M. S. Thesis, San Diego State University, 140pp.

Wesnousky, S. (1986). Earthquakes, Quaternary faults, and seismic hazard in California, J. Geophys. Res. 91, 12,587-12,631.

West, R.B. (1987). Tectonic geomorphology of the Mount Soledad segment of the Rose Canyon fault zone, unpublished senior thesis, San Diego State University.

Youngs, R. R. and K. J. Coppersmith (1985). Implications of fault slip rates and earthquake recurrence models to probabilistic seismic hazard estimates, Bull. Seism. Soc. Am. 75, 939-964.

Youngs, R. R., F. H. Swan, M. S. Power, D. P. Schwartz, and R. K. Green (1987). Probabilistic analysis of earthquake ground shaking hazard along the Wasatch Front, Utah, Report by Geomatrix Consultants, San Francisco, Calif. U.S.G.S. Professional Paper (in press).

APPENDIX I

Listing of earthquakes to affect San Deigo
January 1, 1932 - October 30, 1986

Source: California Institute of Technology

Selection Criteria:
M_L > 5.0
Predicted Amax (Joyner & Boore, 1981) >2.0 cm/sec^2
Prediction for downtown San Diego (32.72 N, -117.15 W)

year	mo	d	hr	mn	sec	lat	long	ML	dist km	amax cm/sec^2
1933	3	11	1	54	7.8	33.617	-117.967	6.3	125.0	13.3
1933	3	11	2	9	0.0	33.750	-118.083	5.0	143.3	4.9
1933	3	11	2	30	0.0	33.750	-118.083	5.1	143.3	5.2
1933	3	11	3	23	0.0	33.750	-118.083	5.0	143.3	4.9
1933	3	11	5	10	22.0	33.700	-118.067	5.1	138.0	5.6
1933	3	11	5	18	4.0	33.575	-117.983	5.2	122.4	7.3
1933	3	11	6	58	3.0	33.683	-118.050	5.5	135.6	7.3
1933	3	11	8	54	57.0	33.700	-118.067	5.1	138.0	5.6
1933	3	11	9	10	0.0	33.750	-118.083	5.1	143.3	5.2
1933	3	11	14	25	0.0	33.850	-118.267	5.0	162.4	3.9
1933	3	13	13	18	28.0	33.750	-118.083	5.3	143.3	5.9
1933	3	14	19	1	50.0	33.617	-118.017	5.1	127.9	6.4
1933	10	2	9	10	17.6	33.783	-118.133	5.4	149.0	5.8
1934	11	25	8	18	0.0	32.083	-116.667	5.0	84.1	11.9
1934	12	30	13	52	0.0	32.280	-115.460[1]	6.5	165.7	8.9
1934	12	31	18	45	0.0	32.140	-114.950[1]	7.1	216.1	7.1
1935	2	24	1	45	0.0	31.940	-116.140[1]	6.0	128.5	10.7
1935	4	29	20	8	0.0	31.750	-116.500	5.0	123.9	6.4
1935	9	8	17	3	0.0	32.900	-115.217	5.0	182.0	3.1
1935	10	11	14	6	0.0	32.900	-115.217	5.0	182.0	3.1
1935	10	24	14	48	7.6	34.100	-116.800	5.1	156.4	4.4
1935	12	20	7	45	0.0	33.167	-115.500	5.0	161.7	3.9
1937	2	27	1	29	18.4	31.867	-116.571[2]	5.0	109.3	7.9
1937	3	25	16	49	1.8	33.465	-116.415[2]	6.0	107.4	14.4
1938	5	31	8	34	55.4	33.699	-117.511	5.5	113.6	9.9
1938	6	6	2	42	0.0	32.900	-115.217	5.0	182.0	3.1
1939	5	1	23	53	0.0	32.000	-117.500	5.0	86.4	11.4
1939	6	24	16	27	0.0	32.000	-117.500	5.0	86.4	11.4
1940	5	18	5	3	58.5	34.083	-116.300	5.4	170.3	4.5
1940	5	18	5	51	20.3	34.067	-116.333	5.2	167.3	4.1
1940	5	18	7	21	32.7	34.067	-116.333	5.0	167.3	3.7
1940	5	19	4	36	40.9	32.733	-115.500	6.7	154.7	11.3
1940	5	19	4	55	0.0	32.767	-115.483	5.5	156.3	5.6
1940	5	19	5	51	34.0	32.767	-115.483	5.5	156.3	5.6
1940	5	19	6	33	20.0	32.767	-115.483	5.0	156.3	4.2
1940	5	19	6	35	40.0	32.767	-115.483	5.5	156.3	5.6
1940	6	4	10	35	8.3	33.000	-116.433	5.1	73.8	15.2
1940	12	7	22	16	27.0	31.667	-115.083	6.0	228.2	3.3
1941	1	9	10	28	42.0	31.700	-115.100	5.5	224.9	2.6
1941	11	14	8	41	36.3	33.783	-118.250	5.4	155.8	5.3
1942	3	3	1	3	24.0	34.000	-115.750	5.0	192.1	2.8
1942	5	23	15	47	29.0	32.983	-115.983[2]	5.0	112.9	7.5
1942	10	21	16	22	13.0	33.049	-116.088[2]	6.5	105.6	19.7
1942	10	21	16	25	19.0	32.967	-116.000	5.0	110.9	7.7
1942	10	21	16	26	54.0	32.967	-116.000	5.0	110.9	7.7
1942	10	22	1	50	38.0	33.233	-115.717	5.5	145.2	6.4
1942	10	22	18	13	26.0	32.967	-116.000	5.0	110.9	7.7
1943	8	29	3	45	13.0	34.267	-116.967	5.5	172.4	4.6
1943	12	22	15	50	28.0	34.333	-115.800	5.5	217.8	2.8
1944	6	12	10	45	34.7	33.976	-116.721	5.1	144.9	5.1
1944	6	12	11	16	36.0	33.994	-116.712	5.3	147.0	5.6
1945	3	20	21	55	7.0	34.250	-116.167[1]	5.0	192.4	2.8
1945	5	12	7	33	0.0	31.630	-115.610[1]	5.2	188.8	3.2
1945	8	15	17	56	24.0	33.217	-116.133	5.7	109.6	11.7
1946	1	8	18	54	18.0	33.000	-115.833	5.4	126.9	7.7
1946	7	18	14	27	58.0	34.533	-115.983	5.6	227.9	2.7
1946	9	28	7	19	9.0	33.950	-116.850	5.0	139.2	5.2
1947	4	10	15	58	6.0	34.983	-116.550	6.2	257.0	2.8
1947	7	24	22	10	46.0	34.017	-116.500	5.5	155.8	5.6
1947	7	25	0	46	31.0	34.017	-116.500	5.0	155.8	4.2
1947	7	25	6	19	49.0	34.017	-116.500	5.2	155.8	4.7
1947	7	26	2	49	41.0	34.017	-116.500	5.1	155.8	4.5
1948	2	24	8	15	10.0	32.500	-118.550	5.3	133.8	6.6
1948	12	4	23	43	17.0	33.933	-116.383	6.5	152.1	10.4
1949	5	2	11	25	47.0	34.017	-115.683	5.9	197.6	4.4
1949	11	4	20	42	38.0	32.180	-116.520	5.7	84.2	17.7
1949	11	5	4	35	24.0	32.200	-116.550	5.1	80.8	13.3
1950	7	28	17	50	48.0	33.117	-115.567	5.4	154.2	5.4
1950	7	29	14	36	32.0	33.117	-115.567	5.5	154.2	5.7
1951	1	24	7	17	2.6	32.983	-115.733	5.6	135.6	7.7
1951	9	2	16	27	32.0	31.000	-117.000	5.2	191.3	3.1
1951	12	26	0	46	54.0	32.817	-118.350	5.9	112.9	12.5
1952	7	21	11	52	14.0	35.000	-119.017	7.7	305.0	4.2
1952	7	21	12	5	31.0	35.000	-119.000	6.4	304.1	2.0
1952	8	23	10	9	7.1	34.519	-118.198	5.0	221.6	2.0
1953	6	14	4	17	29.9	32.950	-115.717	5.5	136.4	7.2
1953	10	10	18	49	6.0	31.800	-116.100	5.0	142.5	5.0
1954	2	1	4	23	57.0	32.300	-115.300	5.2	180.4	3.5
1954	2	1	4	32	2.0	32.300	-115.300	5.6	180.4	4.5
1954	2	1	13	5	29.0	32.300	-115.300[2]	5.1	180.4	3.3
1954	3	19	9	54	29.0	33.296	-116.176[2]	6.2	111.0	15.3

1954	3	19	9	55	56.0	33.283	-116.183	5.0	109.6	7.9
1954	3	19	10	21	17.0	33.283	-116.183	5.5	109.6	10.5
1954	3	23	4	14	50.0	33.283	-116.183	5.1	109.6	8.3
1954	5	31	8	6	24.0	31.600	-115.200	5.2	222.9	2.2
1954	10	17	22	57	18.0	31.500	-116.500	5.7	148.7	6.9
1954	10	24	9	44	8.0	31.730	-115.920[1]	6.0	159.6	7.2
1954	10	24	11	21	24.0	31.500	-116.000	5.4	173.9	4.3
1954	11	12	12	26	47.0	31.770	-115.970[1]	6.3	153.1	9.2
1954	11	12	13	16	42.0	31.500	-116.000	5.0	173.9	3.4
1954	11	14	5	36	19.0	31.500	-116.000	5.4	173.9	4.3
1955	4	25	10	43	8.0	32.333	-115.000	5.2	206.9	2.6
1955	11	26	17	36	0.0	31.600	-116.100	5.4	159.2	5.1
1955	12	17	6	7	29.0	33.000	-115.500	5.4	157.3	5.2
1956	2	9	14	32	38.0	31.750	-115.917	6.8	158.8	11.4
1956	2	9	14	34	0.0	31.700	-115.900	5.6	163.8	5.4
1956	2	9	15	1	33.3	31.600	-115.700	5.3	185.4	3.5
1956	2	9	15	24	26.0	31.750	-115.917	6.1	158.8	7.6
1956	2	9	16	29	53.3	31.600	-115.700	5.8	185.4	4.7
1956	2	9	16	59	53.0	31.750	-115.917	5.7	158.8	6.1
1956	2	9	18	48	45.0	31.750	-115.917	5.7	158.8	6.1
1956	2	10	4	18	15.0	31.583	-115.667	5.0	189.0	2.9
1956	2	10	15	9	29.0	31.750	-115.917	5.0	158.8	4.1
1956	2	10	18	12	54.0	31.750	-115.917	5.5	158.8	5.4
1956	2	11	2	57	46.0	31.750	-115.917	5.1	158.8	4.3
1956	2	11	5	19	0.0	31.700	-115.900	5.0	163.8	3.8
1956	2	11	6	11	24.0	31.750	-115.917	5.0	158.8	4.1
1956	2	11	6	24	25.0	31.583	-115.667	5.4	189.0	3.6
1956	2	14	14	45	32.0	31.500	-115.500	5.0	207.1	2.4
1956	2	14	18	33	34.0	31.500	-115.500	6.3	207.1	5.0
1956	2	15	1	20	38.0	31.500	-115.500	6.4	207.1	5.2
1956	2	15	2	28	39.0	31.500	-115.500	5.3	207.1	2.8
1956	2	15	7	7	47.0	31.500	-115.500	5.2	207.1	2.6
1956	2	15	8	35	54.0	31.500	-115.500	5.0	207.1	2.4
1956	2	16	8	12	28.0	31.500	-115.500	5.0	207.1	2.4
1956	2	25	8	8	51.0	31.500	-115.500	5.1	207.1	2.5
1956	3	3	18	23	13.0	31.583	-115.667	5.1	189.0	3.0
1956	3	9	0	32	40.0	31.750	-115.917	5.0	158.8	4.1
1956	3	10	14	12	54.0	31.500	-115.500	5.0	207.1	2.4
1956	5	10	11	48	54.0	31.833	-116.000	5.0	146.7	4.7
1956	8	25	15	57	43.0	31.500	-115.500	5.0	207.1	2.4
1956	12	13	13	15	37.0	31.000	-115.000	6.0	280.2	2.0
1957	4	25	21	57	38.7	33.216	-115.808	5.2	136.7	6.0
1957	4	25	22	24	12.0	33.183	-115.850	5.1	131.7	6.1
1957	5	26	15	59	33.6	33.231	-116.005	5.0	120.9	6.7
1958	12	1	3	21	18.0	32.200	-115.850[1]	5.8	134.9	8.7
1958	12	1	3	50	0.0	32.250	-115.750	5.0	141.9	5.0
1958	12	1	6	2	0.0	32.250	-115.750	5.5	141.9	6.7
1962	5	27	1	45	35.0	32.270	-115.810[1]	5.1	135.1	5.8
1963	6	11	15	23	38.3	32.010	-116.120[1]	5.8	124.8	10.0
1963	9	23	14	41	52.6	33.710	-116.925	5.0	111.8	7.6
1964	12	22	20	54	33.2	31.811	-117.131	5.6	100.8	12.7
1965	9	25	17	43	44.1	34.712	-116.503	5.2	228.8	2.1
1966	8	7	17	36	26.7	31.800	-114.500	6.3	270.9	2.6
1967	9	21	0	1	54.6	31.426	-115.953	5.2	183.1	3.4
1968	4	9	2	28	59.1	33.190	-116.129	6.4	108.6	17.8
1968	4	9	3	3	53.5	33.113	-116.038	5.2	112.6	8.4
1969	4	28	23	20	42.9	33.343	-116.346	5.8	101.9	14.0
1969	6	10	3	41	32.7	31.625	-116.211	5.0	150.6	4.5
1969	10	24	8	29	12.1	33.291	-119.193	5.1	200.5	2.7
1970	9	12	14	30	53.0	34.270	-117.540	5.4	175.6	4.2
1971	2	9	14	0	41.8	34.411	-118.401	6.4	220.0	4.6
1971	2	9	14	1	8.0	34.411	-118.401	5.8	220.0	3.2
1971	2	9	14	2	44.0	34.411	-118.401	5.8	220.0	3.2
1971	2	9	14	10	28.0	34.411	-118.401	5.3	220.0	2.4
1971	2	9	14	43	46.7	34.308	-118.454	5.2	213.1	2.5
1971	9	30	22	46	11.3	33.033	-115.821	5.1	129.0	6.3
1973	2	21	14	45	57.3	34.065	-119.035	5.9	229.2	3.1
1975	6	1	1	38	49.2	34.516	-116.496	5.2	208.0	2.6
1975	7	17	18	24	47.0	31.927	-115.777	5.0	156.8	4.2
1976	1	10	12	58	15.8	32.084	-115.471	5.0	173.5	3.4
1978	5	5	21	3	15.8	32.211	-115.304	5.2	183.0	3.4
1979	1	1	23	14	38.9	33.944	-118.681	5.0	196.2	2.6
1979	3	15	21	7	16.5	34.327	-116.445	5.2	189.7	3.2
1979	10	15	23	16	53.4	32.614	-115.318	6.6	172.3	8.7
1979	10	15	23	19	30.0	32.766	-115.441	5.2	160.2	4.5
1979	10	16	5	49	10.2	32.927	-115.540	5.1	152.4	4.7
1979	10	16	6	19	48.7	32.928	-115.539	5.1	152.4	4.7
1979	10	16	6	58	42.8	33.014	-115.555	5.5	152.5	5.9
1980	2	25	10	47	38.5	33.501	-116.513	5.5	104.9	11.2
1980	6	9	3	28	19.4	32.185	-115.076	6.1	204.4	4.5
1981	4	26	12	9	28.4	33.098	-115.632	5.7	147.8	7.0
1981	9	4	15	50	50.3	33.671	-119.111	5.3	210.3	2.7
1985	5	8	23	40	20.8	31.890	-115.821	5.0	155.8	4.2
1986	7	8	9	20	44.5	33.998	-116.606	5.6	150.4	6.4
1986	7	13	13	47	8.2	32.971	-117.870	5.3	72.8	17.4
1986	10	29	02	38	25.2	32.616	-117.134	4.7	11.6	93.3